

# Weak gravitational lensing

Matthias Bartelmann

Matteo Maturi

Universität Heidelberg, Zentrum für Astronomie, Institut für Theoretische Astrophysik

Invited and refereed contribution to Scholarpedia

## Abstract

According to the theory of general relativity, masses deflect light in a way similar to convex glass lenses. This gravitational lensing effect is astigmatic, giving rise to image distortions. These distortions allow to quantify cosmic structures statistically on a broad range of scales, and to map the spatial distribution of dark and visible matter. We summarise the theory of weak gravitational lensing and review applications to galaxies, galaxy clusters and larger-scale structures in the Universe.

## 1 Brief historical outline of gravitational lensing

### 1.1 Newton and Soldner

As early as in 1704, Sir Isaac Newton had surmised that light might be deflected by gravity. In his book “Opticks: or, a treatise of the reflections, refractions, inflections and colours of light”, he collected a whole list of questions in an appendix, the first of which was: “Do not Bodies act upon Light at a distance, and by their action bend its Rays; and is not this action (caeteris paribus) strongest at the least distance?” [1]

In Newtonian physics, however, this question cannot even be confidently addressed. Light can be considered as a stream of particles, the photons, which however have no rest mass. In the view of special relativity, photons acquire inertia by their motion, and this inertia contributes to their mass. However, if they could be at rest, no inertia and thus no mass would remain. But gravity should not be able to act on something without mass, or should it?

On the other hand, in Newtonian physics, the trajectory of a small test body around a large mass does not at all depend on the mass of the test body. As Galileo had noticed already, all bodies fall equally rapidly, provided that no forces besides gravity act upon them. If one imagines a light particle with even a tiny mass, its motion e.g. around the Sun would be calculable without problems. If this mass would be halved, the trajectory would remain the same. And what happened if its mass was progressively reduced until it finally completely disappeared?

The astronomer Johann Georg von Soldner was fully aware of this difficulty when he wrote his article “On the deflection of a light ray from its straight motion by the attraction of a heavenly body which it passes closely” for the *Astronomical Almanac* for the year 1804. Assuming that a mass could (and should) be assigned to the (then hypothetical) particles of light, he calculated by what amount such light rays would be deflected that, as seen from the Earth, would just graze the Solar

rim. Almost apologetically, he wrote: “Hopefully nobody will find it questionable that I treat a light ray perfectly as a heavy body. For that light rays have all the absolute properties of matter is seen by the phenomenon of aberration, which is possible only by light rays being indeed material. – And besides, nothing can be conceived that exists and acts on our senses without having the properties of matter.” [2, originally in German, our translation]

### 1.2 Einstein’s two deflection angles

In Einstein’s perception of the essence of gravity, however, this problem does not even exist. Einstein’s theory of general relativity no longer interprets gravity as a force in the Newtonian sense, but explains the effects of gravity on the motion of bodies by the curvature of space-time caused by the presence of matter or energy.

In the framework of an unfinished version of the theory of general relativity, Einstein calculated the deflection of light at the rim of the Sun for the first time in 1911. He found: “A light ray passing the Sun would accordingly suffer a deflection of the magnitude  $4 \cdot 10^{-6} = 0.83$  arc seconds.” [3] This was exactly the same value that Johann Georg von Soldner had found by his calculation within Newtonian physics. The second time, in 1916, Einstein arrived at the conclusion: “A light ray passing the Sun thus experiences a deflection of 1.7 arc seconds.” [4, originally in German, our translation] His value had plainly doubled, and for a good reason: Only within the final theory of general relativity did Einstein find that he needed to account for temporal as well as spatial curvature of space-time by gravity, and this caused precisely twice the amount of light deflection to occur.

This value of 1.7 arc seconds, twice as large as expected from the Newtonian calculation, was confirmed shortly thereafter by observations. During a total Solar eclipse on May 29, 1919, two British expeditions succeeded in measuring the angle by which such stars appeared pushed away from the Sun which happened to be close to the Sun at the moment of the eclipse and became momentarily visible while the Sun was obscured. In November 1919, the authors Dyson, Eddington and Davidson reported: “Thus the results of the expeditions to Sobral and Principe can leave little doubt that a deflection of light takes place in the neighbourhood of the Sun and that it is of the amount demanded by Einstein’s general theory of relativity, as attributable to the sun’s gravitational field.” [5]

On October 9, 1919, Einstein himself had reported in a brief note: “According to a telegram addressed to the signatory by Prof. Lorentz, the English expedition under Eddington, sent out to observe the Solar eclipse of May 29, has observed the

deflection of light at the rim of the Sun required by the general theory of relativity. The value provisionally deduced so far falls between 0.9 and 1.8 arc seconds. The theory demands 1.7 arc seconds.” [6, originally in German, our translation]

### 1.3 Mandl and Zwicky

Even though, for Einstein himself, the deflection of light at the rim of the Sun marked a confirmation of his theory of general relativity, he was sure that this effect would hardly ever gain astrophysical relevance, not to speak of an even more practical importance. When the Czech engineer Rudi W. Mandl visited Einstein in Princeton in 1936 and asked him to calculate the gravitational lensing effect of a star on a more distant star, Einstein finally consented to publish a note on this phenomenon [7], which he however believed to be unobservable. Indirectly also stimulated by Mandl, the Swiss-American astronomer Fritz Zwicky, however, voiced the idea in 1937 that entire clusters of galaxies could act as gravitational lenses [8]. Only four years earlier, Zwicky had found the first indication of dark matter by observations of the Coma galaxy cluster [9]. Nonetheless, it took until 1979 for the first gravitational lens to be found [10]. This lens is a galaxy embedded into a group of galaxies whose gravitational-lensing effect turns a bright, approximately point-like, very distant object, a so-called quasi-stellar object or QSO, into two images.

## 2 Deflection angle and lensing potential

### 2.1 Index of refraction and Fermat’s principle

There are multiple ways at gravitational lensing which agree in the limit which is commonly applied. In by far the most astrophysical applications, the Newtonian gravitational potential  $\Phi$  is small,  $|\Phi|/c^2 \ll 1$ , and the lensing mass distribution moves slowly with respect to the cosmological rest frame. In a galaxy cluster, for example,  $|\Phi|/c^2 \lesssim 10^{-5}$ , and cosmic structures have typical peculiar velocities  $v \lesssim 600 \text{ km s}^{-1} \ll c$ . The standard approach to gravitational lensing has been laid out in several reviews, lecture notes and a text book [11, 12, 13, 14, 15, 16, 17].

Under such conditions, gravitational lensing can be described by a small perturbation of the locally Minkowskian space-time of an observer co-moving with the gravitational lens. The Minkowski metric of special relativity, expressed by its line element

$$ds^2 = -c^2 dt^2 + d\vec{x}^2, \quad (1)$$

is perturbed by the dimension-less Newtonian gravitational potential  $\Phi/c^2$  as

$$ds^2 = -c^2 \left(1 + \frac{2\Phi}{c^2}\right) dt^2 + \left(1 - \frac{2\Phi}{c^2}\right) d\vec{x}^2. \quad (2)$$

With the propagation condition for light,  $ds = 0$ , this expression can be rearranged to find the effective light speed in a weak gravitational field,

$$c' = \left| \frac{d\vec{x}}{dt} \right| = c \left(1 + \frac{2\Phi}{c^2}\right), \quad (3)$$

where  $\Phi/c^2 \ll 1$  was used in a first-order Taylor expansion. Introducing the index of refraction  $n$  by the conventional definition  $c' = c/n$ , we see that a weak gravitational field has the

effective index of refraction

$$n = \frac{c}{c'} = 1 - \frac{2\Phi}{c^2}. \quad (4)$$

Since the gravitational potential is negative if conventionally normalised such as to vanish at infinity, this index of refraction is larger than unity.

We can now apply *Fermat’s principle*, which asserts that a light ray follows that path between two fixed points  $A$  and  $B$  along which its optical path  $\tau$  is extremal,

$$\delta\tau = \delta \int_A^B \frac{c}{n} dt = 0. \quad (5)$$

The variation of  $\tau$  with respect to the light path leads directly to the deflection angle

$$\hat{\alpha} = -\frac{2}{c^2} \int \vec{\nabla}_\perp \Phi d\lambda, \quad (6)$$

which is the gradient of the dimension-less Newtonian potential perpendicular to the light ray, integrated along the light ray and multiplied by two. This factor of two comes from the fact that the perturbed Minkowski metric has equal perturbations in both its temporal and spatial components, as mentioned above in the context of Einstein’s two calculations.

### 2.2 The Born approximation

The integral over the actual light path is complicated to carry out. However, since typical deflection angles are on the order of arc seconds or smaller, the integration path can be approximated by a straight line, just as in the *Born approximation* familiar from quantum mechanics. Then, assuming a point mass  $M$  at the origin of a coordinate system and a light ray propagating parallel to the  $z$  axis and passing the point mass at an impact parameter  $b$ , the deflection angle according to (6) is

$$\hat{\alpha} = -\frac{2}{c^2} \frac{\partial}{\partial b} \int_{-\infty}^{\infty} dz \frac{GM}{\sqrt{b^2 + z^2}} = \frac{4GM}{bc^2} = \frac{2R_S}{b}, \quad (7)$$

where  $R_S = 2GM/c^2$  is the Schwarzschild radius of the lensing point mass. For the Sun, with its mass of  $M = 2 \cdot 10^{33} \text{ g}$ , the Schwarzschild radius is  $R_{S_\odot} \approx 3 \text{ km}$ , hence the deflection angle at the Solar radius  $R_\odot = 7 \cdot 10^5 \text{ km}$  is

$$\hat{\alpha}_\odot \approx \frac{6}{7 \cdot 10^5} \approx 8.6 \cdot 10^{-6} \approx 1.7'' . \quad (8)$$

This is Einstein’s famous result, tested and verified by Dyson, Eddington and Davidson in 1919.

### 2.3 The lensing potential

If the lensing mass distribution is thin compared to the overall extent of the lens system, the light path from the observer to the source can be approximated by straight lines from the observer to the lens and from there on to the source which enclose the deflection angle. This is called the *thin-lens approximation*. It is appropriate for the description of isolated lenses such as galaxy clusters, but inadequate for extended lenses such as the large-scale structures of the Universe. We shall proceed with the thin-lens approximation for now and later generalise the results to extended mass distributions.

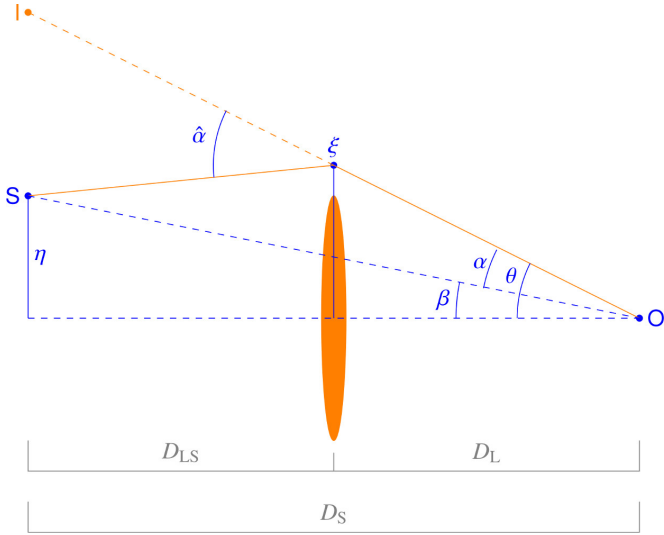


Figure 1: Sketch of a gravitational-lens system (adapted from [12]): The optical axis runs from the observer O through the centre of the lens. The angle between the source S and the optical axis is  $\beta$ , the angle between the image I and the optical axis is  $\theta$ . The light ray towards the image is bent by the deflection angle  $\hat{\alpha}$ , measured at the lens. The reduced deflection angle  $\alpha$  is measured at the observer.

Tracing a light ray back from the observer to the source, the lens or ray-tracing equation can then simply be found from the intercepts of the light ray relative to the (arbitrary) optical axis at the distances of the lens and the source from the observer,  $D_L$  and  $D_S$ , respectively. Let the angles between the optical axis and the image, and between the optical axis and the source on the observer's sky be  $\vec{\theta}$  and  $\vec{\beta}$ , respectively. These angles are vectors because they have a direction as well as a magnitude. Then,

$$D_S \vec{\beta} = D_S \vec{\theta} - D_L \hat{\alpha}, \quad (9)$$

with  $D_{LS}$  being the distance between the lens and the source (cf. Fig. 1). This equation may look trivial, but it is not. It only holds because even in the curved space-time of the Universe, distances can be introduced in such a way that the intercept theorem familiar from Euclidean geometry continues to hold. These are the *angular-diameter distances*. Dividing by  $D_S$  and introducing the *reduced deflection angle*

$$\vec{\alpha} := \frac{D_{LS}}{D_S} \hat{\alpha} \quad (10)$$

leads to the lens or ray-tracing equation in its simplest form,

$$\vec{\beta} = \vec{\theta} - \vec{\alpha}. \quad (11)$$

With Eq. (6), the reduced deflection angle can be written as a gradient,

$$\vec{\alpha} = \vec{\nabla}_\perp \left[ \frac{2}{c^2} \frac{D_{LS}}{D_S} \int \Phi dz \right]. \quad (12)$$

It is convenient to introduce the quantities describing gravitational lensing, such as the reduced deflection angle or the lensing potential, as functions on the sky, i.e. as functions of the angular position  $\vec{\theta}$  on the celestial sphere. Then, gradients need to be taken with respect to angles rather than perpendicular distances. The perpendicular gradient  $\vec{\nabla}_\perp$  occurring in (6) and

(12) is then replaced by the gradient  $\vec{\nabla}_\theta$  with respect to the angle  $\vec{\theta}$  according to

$$\vec{\nabla}_\perp = D_L^{-1} \vec{\nabla}_\theta. \quad (13)$$

The distance  $D_L$  from the observer to the lens appears here because, in the small-angle approximation, the perpendicular separation from the line-of-sight is  $D_L \vec{\theta}$ . Thus, (12) turns into

$$\vec{\alpha} = \vec{\nabla}_\theta \psi \quad \text{with} \quad \psi := \frac{2}{c^2} \frac{D_{LS}}{D_L D_S} \int \Phi dz. \quad (14)$$

The quantity  $\psi$  defined here is called the *lensing potential*. In by far the most situations of astrophysical interest, the lensing potential incorporates all imaging properties of a gravitational lens.

For a point-mass lens, we have seen in (7) that the deflection angle  $\hat{\alpha}$  is proportional to the inverse impact parameter,  $b^{-1}$ . Converting  $b$  to the angle  $\theta$  by  $b = D_L \theta$  and the deflection angle  $\hat{\alpha}$  to the reduced deflection angle  $\alpha$ , we find

$$\alpha = \frac{\partial \psi}{\partial \theta} \quad \text{with} \quad \psi = \frac{4GM}{c^2} \frac{D_{LS}}{D_L D_S} \ln |\theta|, \quad (15)$$

showing that the lensing potential of a point-mass lens at the coordinate origin is proportional to the logarithm of the angular radius.

## 3 Magnification and distortion

### 3.1 The convergence

Taking the divergence of  $\vec{\alpha}$  leads to the Laplacian of  $\psi$ ,

$$\vec{\nabla}_\theta \cdot \vec{\alpha} = \vec{\nabla}_\theta^2 \psi = \frac{2}{c^2} \frac{D_L D_{LS}}{D_S} \int \vec{\nabla}_\perp^2 \Phi dz, \quad (16)$$

where we have replaced the Laplacian  $\vec{\nabla}_\theta^2$  with respect to the angle  $\vec{\theta}$  by the perpendicular Laplacian  $\vec{\nabla}_\perp^2$  with respect to physical coordinates. If we could replace the perpendicular by the complete Laplacian,

$$\vec{\nabla}^2 = \vec{\nabla}_\perp^2 + \frac{\partial^2}{\partial z^2}, \quad (17)$$

we could insert *Poisson's equation*

$$\vec{\nabla}^2 \Phi = 4\pi G \rho \quad (18)$$

into (16). We can indeed do so if the gradient of the potential  $\Phi$  along the line-of-sight, taken at the beginning and at the end of the line-of-sight, can be neglected,

$$\int \frac{\partial^2 \Phi}{\partial z^2} dz = \frac{\partial \Phi}{\partial z} \Big|_{\text{end points}} = 0. \quad (19)$$

This is indeed excellently satisfied in all situations where the extent of the lensing mass distribution is small compared to the cosmological distances  $D_L$ ,  $D_{LS}$  and  $D_S$  characterising the geometry of the lens system.

We thus substitute the complete, three-dimensional Laplacian for the two-dimensional, perpendicular Laplacian in (16) and use Poisson's equation to write

$$\vec{\nabla}_\theta^2 \psi = \frac{8\pi G}{c^2} \frac{D_L D_{LS}}{D_S} \Sigma, \quad (20)$$

where the *surface mass density*

$$\Sigma := \int \rho \, dz \quad (21)$$

is defined as the line-of-sight projection of the three-dimensional mass density  $\rho$ . The prefactor

$$\frac{4\pi G}{c^2} \frac{D_L D_{LS}}{D_S} =: \Sigma_{\text{cr}}^{-1} \quad (22)$$

has the dimension of an inverse surface-mass density,  $\text{cm}^2 \text{g}^{-1}$ . The quantity  $\Sigma_{\text{cr}}$  is called *critical surface mass density*. With these definitions,

$$\vec{\nabla}_\theta^2 \psi = 2 \frac{\Sigma}{\Sigma_{\text{cr}}} =: 2\kappa, \quad (23)$$

where we introduced the dimension-less surface-mass density or *convergence*  $\kappa$ . From here on, we shall drop the subscript  $\theta$  on the gradient, understanding that  $\vec{\nabla}$  is the gradient  $\vec{\nabla}_\theta$  with respect to  $\vec{\theta}$ .

### 3.2 Geometrical sensitivity of gravitational lensing

The Poisson equation (23) shows that the source of the lensing potential  $\psi$  is twice the dimension-less convergence or surface-mass density  $\kappa$ , i.e. the surface-mass density  $\Sigma$  of the lens divided by its critical surface mass density  $\Sigma_{\text{cr}}$ . A mass distribution with a fixed surface-mass density  $\Sigma$  can thus be a more or less efficient gravitational lens, depending on the overall extent of the lens system composed of observer, source, and lens, and depending on where the lens is located along the line-of-sight. Lensing is most efficient where the critical surface-mass density  $\Sigma_{\text{cr}}$  is minimal, or where the expression in (22) is maximal. In Euclidean space, this would be half-way between the observer and the source. In the curved space-time of our Universe, the location of maximal lensing sensitivity is somewhat closer in redshift to the observer. The geometrical sensitivity of gravitational lensing is one of the main characteristics turning lensing into a powerful tool for cosmology.

### 3.3 Linearised lens mapping and Jacobi matrix

In terms of the lensing potential  $\psi$ , the lens equation (11) is

$$\vec{\beta} = \vec{\theta} - \vec{\nabla} \psi. \quad (24)$$

Imagine now a source substantially smaller than any typical scale of variation in the deflection angle. Let  $\delta\vec{\beta}$  the angular separation of a point on an outer source contour from the centre of the source. Then, the corresponding angular distance of the image point can be approximated by a first-order Taylor expansion of the lens equation (24),

$$\delta\vec{\beta} \approx \mathcal{A} \delta\vec{\theta}, \quad (25)$$

where  $\mathcal{A}$  is the *Jacobian matrix* of the lens mapping. It has the components

$$\mathcal{A}_{ij} = \frac{\partial \beta_i}{\partial \theta_j} = \delta_{ij} - \psi_{ij}, \quad (26)$$

where the potential derivatives are to be taken at the centre of the lensed image. Here, we have introduced the common short-hand notation

$$\psi_{ij} := \frac{\partial^2 \psi}{\partial \theta_i \partial \theta_j} \quad (27)$$

for the second partial derivatives of  $\psi$ .

Equations (25) and (26) are interesting expressions. First, (25) states that the Jacobi matrix  $\mathcal{A}$  maps small distances  $\delta\vec{\theta}$  in an image back to small distances  $\delta\vec{\beta}$  in the source. This is the foundation of by far the most applications of weak gravitational lensing in astrophysics and cosmology. Equation (26) shows that, in the absence of the lensing potential, the lens mapping is simply the identity. In the presence of a lens, the local properties of the lens mapping are determined by the curvature of the lensing potential  $\psi$ , expressed by the matrix of second derivatives of  $\psi$ , or the Hessian matrix of the potential. Second derivatives of gravitational potentials are tidal forces. Locally, deformations by the lens mapping are thus determined by the gravitational tidal forces caused by the lens.

### 3.4 Shear and magnification

For the physical interpretation of the Jacobi matrix  $\mathcal{A}$ , it is convenient and instructive to split  $\mathcal{A}$  into an isotropic and an anisotropic, trace-free part by taking the trace,

$$\text{tr} \mathcal{A} = 2 - \vec{\nabla}^2 \psi = 2(1 - \kappa), \quad (28)$$

and subtracting it from  $\mathcal{A}$  by means of the unit matrix  $\mathcal{I}$  to obtain the shear matrix

$$\Gamma := - \left( \mathcal{A} - \frac{1}{2} (\text{tr} \mathcal{A}) \mathcal{I} \right) \quad (29)$$

which has the components

$$\begin{aligned} \Gamma_{11} =: \gamma_1 &= \frac{1}{2} (\psi_{11} - \psi_{22}), & \Gamma_{22} &= -\gamma_1, \\ \Gamma_{12} = \Gamma_{21} =: \gamma_2 &= \psi_{12}. \end{aligned} \quad (30)$$

These manipulations leave the Jacobi matrix in the form

$$\mathcal{A} = (1 - \kappa) \mathcal{I} - \Gamma = \begin{pmatrix} 1 - \kappa - \gamma_1 & -\gamma_2 \\ -\gamma_2 & 1 - \kappa + \gamma_1 \end{pmatrix}. \quad (31)$$

The linearised lens equation (25) tells us the inverse of what we typically want to know from weak gravitational lensing. Since we observe images but cannot access the sources, we need to infer the separation  $\delta\vec{\theta}$  of image points from the image centre. If the Jacobi matrix  $\mathcal{A}$  has a non-vanishing determinant, it can be inverted, allowing us to write

$$\delta\vec{\theta} = \mathcal{A}^{-1} \delta\vec{\beta}. \quad (32)$$

The inverse Jacobi matrix determines how sources are mapped on images. In weak gravitational lensing, the Jacobi determinant

$$\det \mathcal{A} = (1 - \kappa)^2 - \gamma^2 \quad (33)$$

with

$$\gamma^2 := \gamma_1^2 + \gamma_2^2 \quad (34)$$

is near unity because the absolute values of the convergence  $\kappa$  and the shear  $\gamma$  are both small compared to unity. Points in the lens where  $\det \mathcal{A} = 0$  are called critical points. They play no role in weak gravitational lensing but are centrally important for strong lensing.

Thus, we can always assume in weak gravitational lensing that the linear lens mapping is invertible. The inverse of the Jacobi matrix is

$$\mathcal{A}^{-1} = \frac{1}{\det \mathcal{A}} \begin{pmatrix} 1 - \kappa + \gamma_1 & \gamma_2 \\ \gamma_2 & 1 - \kappa - \gamma_1 \end{pmatrix}. \quad (35)$$

The prefactor in this expression indicates that the solid angle spanned by the image is changed compared to the solid angle covered by the source by the *magnification factor*

$$\mu = \frac{1}{\det \mathcal{A}} = \frac{1}{(1 - \kappa)^2 - \gamma^2} \approx 1 + 2\kappa, \quad (36)$$

where the final approximation is a first-order Taylor expansion. Thus, in weak lensing, the magnification of an image is essentially (i.e. to first Taylor order) determined by the convergence  $\kappa$ , not by the shear.

### 3.5 Image distortion

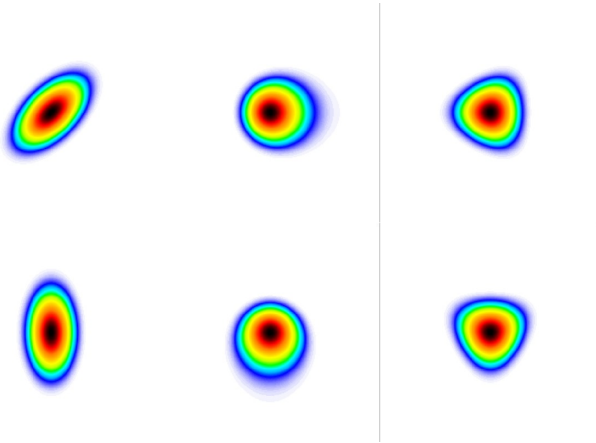


Figure 2: Illustration of gravitational-lensing effects on small sources: The left column shows the effects of both components of the shear on a circular source. The middle and right columns illustrate effects of higher order, quantified by the so-called flexion components  $\mathcal{F}$  and  $\mathcal{G}$ , which are linear combinations of third potential derivatives.  $\mathcal{F}$  flexion leads to a centroid shift while  $\mathcal{G}$  flexion causes a triangular deformation.

The eigenvalues of the inverse Jacobi matrix  $\mathcal{A}^{-1}$  are

$$\lambda_{\pm} = \frac{1 - \kappa \pm \gamma}{\det \mathcal{A}} = \frac{1}{1 - \kappa \mp \gamma}. \quad (37)$$

A hypothetical circular source is deformed by weak gravitational lensing to become an ellipse whose semi-major and semi-minor axes, called  $a$  and  $b$ , respectively, are proportional to the eigenvalues  $\lambda_{\pm}$ . By its common definition, the *ellipticity*  $\varepsilon$  of such an image is

$$\varepsilon := \frac{a - b}{a + b} = \frac{\lambda_+ - \lambda_-}{\lambda_+ + \lambda_-} = \frac{\gamma}{1 - \kappa}. \quad (38)$$

Since the source size prior to lensing is typically inaccessible to observation, the magnification of an image relative to the source cannot directly be measured. The ellipticity  $\varepsilon$  and the orientation of elliptically distorted images are thus the only information supplied by weak lensing in the vast majority of cases. Equation (38) shows that the ellipticity is determined by the so-called *reduced shear*

$$g = \frac{\gamma}{1 - \kappa} \quad (39)$$

rather than by the shear itself. If  $\kappa \ll 1$  which can most often be assumed in cases of weak lensing,  $\varepsilon = g \approx \gamma$ . The effects of both shear components on a circular source are illustrated in Fig. 2 together with higher-order distortions.

## 4 Ellipticity measurement

### 4.1 Local averages and angular resolution

The sources typically used in observations of weak gravitational lensing are of course not circular, but intrinsically elliptical. In lowest-order approximation, the intrinsic source ellipticity  $\varepsilon_S$  and the ellipticity caused by lensing add. Then,

$$\varepsilon \approx g + \varepsilon_S. \quad (40)$$

One of the most essential assumptions in the interpretation of weak gravitational lensing is that the intrinsic ellipticities approach zero when averaged over sufficiently large samples,  $\langle \varepsilon_S \rangle \approx 0$ .

Fortunately, the sky is studded with so many faint, distant galaxies that averages over many of them can be taken on angular scales small compared to the typical scales which the shear and the convergence of the lens vary on. On deep images taken with ground-based telescopes (at an  $r$ -band magnitude of  $\sim 25$ ),  $n \approx 10$  galaxies are found per square arc minute, and  $n \approx 30 - 50$  is reached on images taken in space. The standard deviation of the intrinsic ellipticity is measured to be  $\sigma_{\varepsilon} \approx 0.2$  per source. Averaging over  $N$  faint galaxy images, the scatter of the intrinsic ellipticity is reduced to

$$\Delta \langle \varepsilon_S \rangle \approx \frac{\sigma_{\varepsilon}}{\sqrt{N}}, \quad (41)$$

and the angular resolution  $\Delta\theta$  of this measurement is limited by

$$N = \pi \Delta\theta^2 n \quad \text{or} \quad \Delta\theta = \left( \frac{N}{\pi n} \right)^{1/2}. \quad (42)$$

For  $N = 10$ , we find  $\Delta \langle \varepsilon_S \rangle \approx 0.06$  and  $\Delta\theta \approx 1'$ , assuming  $n \approx 10$  source galaxies per square arc minute. It is of paramount importance for weak gravitational lensing to verify that intrinsic source ellipticities do indeed average to zero, or otherwise to quantify the degree to which they do not.

### 4.2 Measurement process

There are essentially two general approaches to the measurement of image ellipticities. Both of them build upon the measured surface brightness  $I(\vec{\theta})$  of an image. In the forward modelling approach, models for the surface brightness of elliptical sources are fit to the image, allowing to read off the model ellipticity once the best fit has been found. In the other, model-free approach, the quadrupole moments  $Q_{ij}$  of the surface brightness are measured,

$$Q_{ij} = \int d^2\theta I(\vec{\theta}) \theta_i \theta_j, \quad i, j = 1, 2. \quad (43)$$

From them, the two components of the ellipticity are

$$\varepsilon_1 = \frac{Q_{11} - Q_{22}}{2N_Q}, \quad \varepsilon_2 = \frac{Q_{12}}{N_Q}, \quad N_Q := \frac{1}{2} \text{tr} Q + \sqrt{\det Q}. \quad (44)$$

Both methods have their advantages and disadvantages. The forward-modelling approach needs to assume a surface-brightness distribution which may or may not reflect the image properties well. Biases in the inferred ellipticities are possible and likely if the model is not well adapted to the image. The measurement of the surface-brightness moments is hampered

by the fact that the formally infinite integral in (43) will pick up intensity fluctuations surrounding the typically faint and small image. To control this noise contribution, a weight function needs to be introduced in (43), effectively limiting the domain of the integral. The inevitable effects of the weight function on the ellipticity measurement need to be corrected afterwards. Alternatively, denoising procedures can be applied to the images.

On the whole, measuring the ellipticities of distant source galaxies accurately is very difficult. Distortions caused by weak lensing are on the order of up to  $\sim 10$  per cent, i.e. the difference of the semi-axes of typical images is only a few per cent of their sum. Ellipticities thus have to be measured either by model fitting or by measuring the quadrupole moments of the surface-brightness distribution from faint, small, pixellised images distorted by weak lensing at the per cent level.

Substantial complications arise because these faint galaxy images are irregular and distorted prior to lensing. Moreover, they are being observed through optical systems with their own small, but numerous and subtle imperfections and physical limitations. Even if small, these imperfections typically imprint noise and systematics on the measured ellipticities which also have to be carefully corrected. In particular, the point-spread function of the telescope optics needs to be carefully determined in order to quantify any distortions caused by the optical system itself. Usually, the point-spread function is estimated from the images of stars in the observed field.

In the course of these developments, algorithms were described and implemented for measuring the weak shear signal from large data fields. The Shear Testing Programme (STEP) was launched to test and improve the accuracy of shear measurements from weakly distorted images of distant galaxies in the presence of several perturbing effects [18, 19].

On the whole, ellipticity measurements must still be considered an art which is under ongoing development [20, 21, 22, 23, 24, 25, 26, 27]. For the purposes of this review, we cannot go into any detail of this complicated and demanding measurement process. Suffice it to say that it belongs to the most fascinating developments in extragalactic astrophysics and cosmology since the turn of the century that highly reliable and significant measurements of weak gravitational lensing by galaxies, galaxy clusters as well as by large-scale structures have routinely become possible.

## 5 Extended lenses

### 5.1 Generalisation of the lensing potential

So far, we have assumed that the lens is geometrically small compared to the overall scale of the lens system. Since this is clearly not appropriate for gravitational lensing by the large-scale structures in our Universe, we need to generalise the results derived so far to the case of extended lenses. To achieve this, it suffices to pull the distance factors in the definition of the lensing potential in (14) under the line-of-sight integral. Before we can meaningfully do so, however, we need to clarify the concept of a distance in cosmology.

In the curved and expanding space-time of our Universe, distances are no longer uniquely defined. Depending on the measurement procedure intended, distances typically turn out to be vastly different. For gravitational lensing, the appropriate

distance measure is defined such that the ratio between the physical size of a small object and its angular extent equals its distance, which is the relation familiar from static Euclidean space. The distance defined this way is called *angular-diameter distance*.

Since our Universe is expanding, spatial separations between any two points grow in time in a way quantified by the so-called scale factor  $a$ . Commonly, the scale factor is normalised to unity at the present cosmic epoch. It is then convenient to introduce so-called *comoving distances*, which are distances defined on a spatial hypersurface constructed at the present time. Measurements have shown that, even though our Universe has a finite space-time curvature, its spatial curvature cannot be distinguished from zero within the measurement uncertainty. In other words, our Universe turns out to be well described as spatially flat.

Let now  $\chi$  be the comoving angular-diameter distance in a spatially flat space-time, then the lensing potential of an extended lens acting on a source at distance  $\chi_S$  is

$$\psi(\vec{\theta}) = \frac{2}{c^2} \int_0^{\chi_S} d\chi \frac{\chi_S - \chi}{\chi_S \chi} \Phi(\chi \vec{\theta}, \chi). \quad (45)$$

Note the similarity to the expression for the lensing potential of a thin lens in (14): the distance prefactor is replaced according to

$$\frac{D_{LS}}{D_L D_S} \rightarrow \frac{\chi_S - \chi}{\chi_S \chi} \quad (46)$$

and pulled under the integral, the line-of-sight integration is being performed over  $d\chi$ , and the Newtonian potential is taken at the position  $\chi \vec{\theta}$  perpendicular and  $\chi$  parallel to the line-of-sight.

### 5.2 Deflection angle, convergence and shear

The remaining quantities, in particular the reduced deflection angle  $\vec{\alpha}$ , the convergence  $\kappa$  and the shear  $\gamma$ , can now be derived from  $\psi$  in the usual manner,

$$\vec{\alpha} = \vec{\nabla} \psi, \quad \kappa = \frac{1}{2} \vec{\nabla}^2 \psi, \quad \gamma_1 = \frac{1}{2} (\psi_{11} - \psi_{22}), \quad \gamma_2 = \psi_{12}, \quad (47)$$

where all derivatives are to be taken with respect to the angular position  $\vec{\theta}$ , as introduced before. In particular, the convergence to be assigned to an extended lens is

$$\kappa = \frac{4\pi G}{c^2} \int_0^{\chi_S} d\chi \frac{\chi(\chi_S - \chi)}{\chi_S} a^2 \rho(\chi), \quad (48)$$

where Poisson's equation was used again after replacing the Laplacian with respect to perpendicular coordinates by the full Laplacian. The squared scale factor  $a^2$  takes into account that we are using comoving angular-diameter distances. Expression (48) shows that the convergence is a geometrically weighted line-of-sight integral over the mass density  $\rho$ . It is important to note, however, that  $\rho$  is the *fluctuation* of the mass density about its cosmological mean value  $\bar{\rho}$  and not the entire mass density. This is because the bending of light by the mean mass density is already incorporated into the distance measure  $\chi$ . The convergence  $\kappa$  from (48) thus describes the lensing effects of matter inhomogeneities in an otherwise homogeneous mean universe.

Introducing the dimension-less *density contrast*  $\delta$  as the density fluctuation about the mean relative to the mean, the density

$\rho$  to be inserted into (48) is  $\rho = \bar{\rho}\delta$ . In terms of conventional cosmological parameters, the mean matter density is

$$\bar{\rho} = \frac{3H_0^2}{8\pi G}\Omega_{m0}a^{-3} = \bar{\rho}_0 a^{-3}, \quad (49)$$

where  $H_0$  is the Hubble constant quantifying the present expansion rate of the universe, and  $\Omega_{m0}$  is the dimension-less matter-density parameter. Inserting (49) into (48) gives the expression

$$\kappa = \frac{3}{2} \frac{H_0^2}{c^2} \Omega_{m0} \int_0^{\chi_s} d\chi \frac{\chi(\chi_s - \chi)}{\chi_s} \frac{\delta(\chi)}{a} \quad (50)$$

for the convergence  $\kappa$  of an extended lens. It is called *effective convergence* because it corresponds to the convergence of a thin lens whose effects are equivalent to those caused by the actual extended matter distribution.

## 6 Cosmological weak gravitational lensing

### 6.1 Limber's approximation

The lensing effects by the cosmic large-scale structures along one particular line-of-sight cannot be predicted because the actual matter distribution in any direction is unknown. What can be predicted, however, is the degree to which lensing quantities such as the lensing potential, the deflection angle, the convergence and the shear are correlated with each other. To give just one example, this means that, if some image distortion by lensing is measured in one particular direction, the image distortion measured in a nearby direction should be similar. The smaller the angle is chosen between the two directions, the more similar the distortions are expected to be, and if the angle becomes large, the distortions should become independent.

This expected behaviour is quantified by an *angular correlation function*. Let  $x(\vec{\theta})$  be a quantity measured on the sky, its angular correlation functions is

$$\xi_x(\varphi) := \langle x(\vec{\theta})x(\vec{\theta} + \vec{\varphi}) \rangle. \quad (51)$$

The average indicated by the angular brackets is quite involved: It combines an average over all positions  $\vec{\theta}$  with an average over all orientations of the separation vector  $\vec{\varphi}$  on the sky. The concept behind assuming that the angular correlation function depends only on the absolute value of  $\varphi$  but not on its orientation is the statistical isotropy of the cosmic large-scale structures: On average, these structures should not identify an orientation on the sky.

In many applications, it is convenient to Fourier-transform the correlation function  $\xi(\varphi)$  to obtain the so-called *angular power spectrum*,

$$C(l) = \int d^2\varphi \xi(\varphi) e^{-i\vec{l}\cdot\vec{\varphi}}. \quad (52)$$

Here,  $\vec{l}$  is the two-dimensional wave vector conjugate to the angular separation  $\vec{\varphi}$ .

Quite often, the weak-lensing power spectra are calculated by means of Limber's approximation. It asserts that, if the quantity  $x(\vec{\theta})$  defined in two dimensions is a projection

$$x(\vec{\theta}) = \int_0^{\chi_s} d\chi w(\chi) y(\chi\vec{\theta}, \chi) \quad (53)$$

of a quantity  $y(\vec{r})$  defined in three dimensions with a weight function  $w(\chi)$ , then the angular power spectrum of  $x$  is given by

$$C_x(l) = \int_0^{\chi_s} d\chi \frac{w^2(\chi)}{\chi^2} P_y\left(\frac{l}{\chi}\right), \quad (54)$$

where  $P_y(k)$  is the power spectrum of  $y$ , taken at the three-dimensional wave number  $k = l/\chi$ . The condition for Limber's approximation to be applicable is that  $y$  must vary on length scales much smaller than the typical length scale of the weight function  $w$ .

### 6.2 Convergence power spectrum

Equation (50) shows that the effective convergence is a projection of the density contrast  $\delta$  with the weight function

$$w(\chi) = \frac{3}{2} \frac{H_0^2}{c^2} \Omega_{m0} \frac{\chi(\chi_s - \chi)}{a\chi_s}. \quad (55)$$

The power spectrum of the convergence  $C_\kappa(l)$  is thus determined by a weighted line-of-sight integral over the power spectrum  $P_\delta(k)$  of the density contrast.

To further clarify the physical interpretation of cosmological weak gravitational lensing, we write the power spectrum  $P_\delta$  in a different way, motivated as follows. As long as the density contrast is small,  $\delta \ll 1$ , it can be shown to increase with time in proportion to a time-dependent linear growth factor  $D_+(a)$ . Being quadratic in the density contrast, the power spectrum thus grows like  $P_\delta \propto D_+^2$  on sufficiently large scales whose wave number  $k$  is sufficiently small. On such scales, the power spectrum  $P_\delta$  keeps its initial shape. On small scales, this shape is changed by non-linear effects on the evolution of the density contrast. Notwithstanding this non-linear complication, we write the power spectrum  $P_\delta$  as a slowly varying shape function  $\mathcal{P}$  times an amplitude. Conventionally, this amplitude is called  $\sigma_8^2$  and set at the present epoch. In terms of the power spectrum linearly extrapolated to the present time,  $\sigma_8$  is defined by

$$\sigma_8^2 = \int_0^\infty \frac{k^2 dk}{2\pi^2} P_\delta(k) W_8^2(k), \quad (56)$$

where  $W_8(k)$  is a filter function suppressing all modes smaller than  $8 h^{-1}$  Mpc. Setting the linear growth factor  $D_+$  to unity at present, the density-fluctuation power spectrum can then be written as

$$P_\delta(k) = \sigma_8^2 D_+^2(a) \mathcal{P}(k). \quad (57)$$

With this expression for  $P_\delta(k)$ , the convergence power spectrum is given by

$$C_\kappa(l) = \frac{9}{4} \left(\frac{H_0}{c}\right)^4 \Omega_{m0}^2 \sigma_8^2 \int_0^{\chi_s} d\chi \left[ \frac{D_+(a)\chi(\chi_s - \chi)}{a\chi_s} \right]^2 \mathcal{P}\left(\frac{l}{\chi}\right). \quad (58)$$

This equation is cosmologically very important. First, the convergence power spectrum  $C_\kappa(l)$  can be measured in a way to be described shortly. Second, the *shape* of the convergence power spectrum depends on the shape  $\mathcal{P}$  of the power spectrum  $P_\delta$  for the density contrast, which can thus be inferred from measurements as well. Third, the *amplitude* of the convergence power spectrum is directly proportional to the squared matter-density parameter times the amplitude of the power spectrum,  $\Omega_{m0}^2 \sigma_8^2$ . Fourth, the weight function appearing in square brackets under the integral in (58) contains the linear

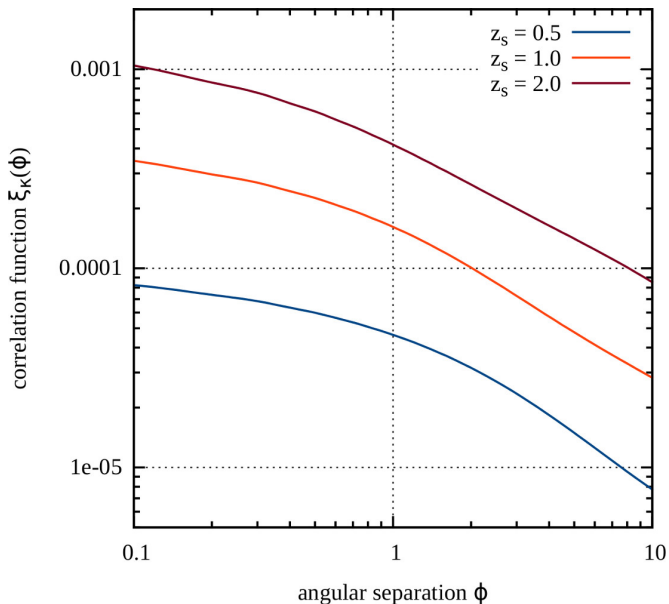


Figure 3: The angular correlation function of the effective convergence is shown for three source redshifts, as a function of the angular separation.

growth factor  $D_+(a)$  of the density contrast, which opens a way towards probing the evolution of cosmic structures with time.

The prefactor  $\Omega_{m0}^2 \sigma_8^2$  is characteristic and has an intuitive meaning as well. The density parameter  $\Omega_{m0}$  quantifies the mean matter density in the universe, while the parameter  $\sigma_8$  quantifies how strongly this matter is clumped. Gravitational lensing alone cannot distinguish between a low density of strongly clumped matter and a high density of weakly clumped matter.

### 6.3 Measurement principle

The convergence  $\kappa$  alone can only be accessed through the magnification, as (36) shows. Measuring the magnification is possible, but difficult. Routinely, cosmological weak lensing is quantified by the shear  $\gamma$ . A simple consideration shows however that shear and convergence have identical power spectra. To see this, we transform the defining equations for  $\kappa$  and  $\gamma$  into Fourier space, where they read

$$2\hat{\kappa} = -l^2 \hat{\psi}, \quad 2\hat{\gamma}_1 = -\left(l_1^2 - l_2^2\right) \hat{\psi}, \quad \hat{\gamma}_2 = -l_1 l_2 \hat{\psi}, \quad (59)$$

with the hats denoting the Fourier transform. Now,

$$4|\hat{\gamma}|^2 = \left[\left(l_1^2 - l_2^2\right)^2 + 4l_1^2 l_2^2\right] |\hat{\psi}|^2 = \left(l_1^2 + l_2^2\right)^2 |\hat{\psi}|^2 = 4|\hat{\kappa}|^2, \quad (60)$$

showing that the shear power spectrum is also given by (58),  $C_\gamma = C_\kappa$ .

Thus, the power spectrum or, equivalently, the correlation function of the weak distortions of distant galaxy images imprinted by cosmological weak lensing needs to be measured. This can be achieved as described in the subsection ‘‘Measurement process’’ above.

### 6.4 Gravitational lensing of the Cosmic Microwave Background

The most distant source of electromagnetic radiation we can observe in our Universe is the so-called Cosmic Microwave

Background (CMB). It was emitted when the cosmic radiation temperature fell to approximately 3000 K and allowed the cosmic plasma to recombine for the first time in cosmic history, approximately 400,000 years after the Big Bang. As neutral atoms were formed, the free charges disappeared, and the cosmic matter became essentially transparent. From then on, the electromagnetic heat radiation left over from the Big Bang could propagate freely through the Universe.

The CMB is cosmologically highly important because, prior to its emission, energy-density fluctuations were imprinted on it by the cosmic structures that had already begun forming. We can observe these primordial energy-density fluctuations as tiny fluctuations of the CMB temperature around its mean. The mean CMB temperature today was measured by the COBE satellite to be 2.726 K, and the relative temperature fluctuations are of order  $10^{-5}$ . Precise measurements of these fluctuations by the COBE, WMAP and Planck satellites as well as by several balloon-borne and ground-based experiments have turned into the major information source on the physical state of the early Universe.

However, with the CMB photons having been released about 400,000 years after the Big Bang, they had to travel through the Universe for almost 14 billion years before they reached our detectors. Doing so, they passed the growing network of cosmic structures and experienced their weak gravitational lensing effects. The photons of the CMB could not propagate along straight lines (or unperturbed null geodesics), but along weakly perturbed paths. What we observe is thus not the CMB itself, but an image of it slightly distorted by gravitational lensing [28].

Gravitational lensing of the CMB is weak and confined to angular scales of approximately 10 arc minutes and less. It can be thought of as a diffusion process slightly blurring the CMB on such angular scales. Fortunately, however, the effects of gravitational lensing on the CMB can be statistically quantified from the data itself, and thus be removed.

The essential reason for this correction to be possible is best seen thinking of a Fourier decomposition of the temperature fluctuation on the CMB. From the origin of these temperature fluctuations, their Fourier modes are independent, i.e. there is intrinsically no correlation between any two CMB temperature-fluctuation Fourier modes with different wave vectors. Through its focusing effect, however, gravitational lensing slightly changes the wave numbers of lensed Fourier modes. Gravitational lensing thus mixes temperature-fluctuation Fourier modes of different wave vectors and thus causes them to be correlated. In the data of the Planck satellite, the weak cosmological lensing effects on the CMB could be measured directly for the first time [29]. The amplitude and the shape of the lensing correlation function inferred from the CMB provide additional strong confirmation for the cosmological standard model.

## 7 Weak gravitational lensing by galaxies and galaxy clusters

### 7.1 Weak lensing of galaxies by galaxies

Less distant galaxies can act as weak gravitational lenses on more distant galaxies. Through their gravitational shear, the lensing galaxies imprint a weak tangential distortion pattern on



the images of the lensed galaxies in their close neighbourhood [30]. This weak shear signal is superposed on the intrinsic ellipticities and irregularities of the background-galaxy images and thus requires statistical techniques for its identification and extraction. (See [31] for a review on strong lensing by galaxies.) Foreground and background galaxies can tentatively be separated according to their apparent brightness. Galaxy-galaxy lensing, as the effect is called, can constrain the potential depth and size of the dark-matter haloes inhabited by the lensing galaxies. First measurements in 1996 found potential depths and halo radii typical for massive galaxies [30, 32].

The statistical signal extraction can be improved by a thorough maximum-likelihood analysis, taking the distance distributions of lensing foreground and lensed background galaxies into account [33]. The galaxy-galaxy lensing signal of galaxies embedded in galaxy clusters could also be detected; it revealed that cluster galaxies are smaller than galaxies outside clusters, with their radius shrinking with the density of the environment [34, 35, 36, 37]. Galaxy-galaxy lensing also reveals that the dark-matter haloes around the lensing galaxies are flattened [38].

Combinations of weak gravitational lensing of galaxies by galaxies with measurements of optical brightness and stellar velocities in galaxies have been used to infer that the dark-matter distribution surrounding galaxies falls off rather steeply towards the outskirts of the dark galaxy haloes. Measurements of galaxy-galaxy lensing in wide-field surveys such as the Sloan Digital Sky Survey, the Las Campanas Redshift Survey or the Canada-France-Hawaii Legacy Survey confirm that bright galaxies have projected density profiles falling with radius  $r$  approximately like  $r^{-1}$ , are characterised by stellar orbital velocities of approximately  $v_c = (150 - 240) \text{ km s}^{-1}$ , are hosted by dark-matter haloes of typically  $(2.7 - 11) \times 10^{11} h^{-1} M_\odot$  and have mass-to-light ratios between  $M/L \simeq 120 h M_\odot/L_\odot$  in blue and  $\simeq 170 h M_\odot/L_\odot$  in red light [39, 40, 41, 42, 43, 44, 45].

The overall dark-matter halo masses range between  $(5 - 10) \times 10^{11} h^{-1} M_\odot$ , the mass-to-light ratio increases gently with luminosity and the mass-to-light ratios of bright spiral galaxies are approximately half those of elliptical galaxies [46, 47]. The masses quoted in this context are typically the total (virial) masses of haloes with parameterised density profiles adapted to the measured lensing signal.

Weak gravitational lensing by galaxies has also been used to study how dark matter and galaxies are correlated on large scales. The correlation function could be measured to separations reaching  $10 h^{-1} \text{ Mpc}$ . It shows a typical correlation length of  $r_0 \simeq (5.4 \pm 0.7) h^{-1} \text{ Mpc}$  and falls off with distance with a approximate power law with exponent  $1.79 \pm 0.05$ . The density contrast in the galaxy distribution may either follow the density contrast in the dark matter, or increase slightly with scale. These results are generally in good agreement with theoretical expectations, except that the mass-to-light ratio found in simulations is typically somewhat too high. Satellite galaxies orbiting the lensing galaxies could be physically aligned with their hosts by the gravitational tidal field and thus mimic a weak galaxy-galaxy lensing signal. On the relevant scales, this possible contamination is probably less than 15% [48, 49, 50, 51, 52, 53].

The availability of huge surveys with sufficient depth and image quality for weak-lensing studies has opened new applications also for galaxy-galaxy lensing. Exciting examples of more detailed studies enabled this way are the measurement

of mean masses of dark-matter haloes hosting active galactic nuclei (AGN), which found that radio-loud AGN reside in host haloes which are typically  $\approx 20$  times more massive than for radio-quiet AGN. Moreover, the combination of galaxy-galaxy lensing with galaxy correlations has been used to specify the mean mass-to-light ratio of the galaxies and to break degeneracies between cosmological parameters [54, 55, 56, 57].

## 7.2 Cluster masses and mass-to-light ratios

As described above, galaxy clusters imprint a coherent weak distortion pattern onto the many faint and distant galaxies in their background. Since those distant galaxies reach number densities of  $\approx 40$  per square arc minute in typical images taken with large ground-based telescopes, typical galaxy clusters thus cover of order  $10^3$  background galaxies.

As shown above, shear and convergence are both related through the scalar lensing potential. Knowing the shear thus allows the scaled surface-mass density to be reconstructed. Cluster convergence maps can be obtained by convolving the measured shear signal with a simple kernel, opening the way to systematic, parameter-free, two-dimensional cluster studies. An immediate application of this technique to the cluster MS 1224 revealed a surprisingly high mass-to-light ratio of  $\approx 800 h M_\odot/L_\odot$ , about four times the typical cluster value [58, 59]

Weaknesses in this convolution algorithm mainly due to the non-locality of the convolution were identified and could be removed [60, 61]. Another, purely local cluster reconstruction method has been proposed based on an entropy-regularised maximum-likelihood approach. This method allows the straightforward extension of the reconstruction algorithm to include all observable quantities provided by galaxy clusters [62, 63, 64, 65, 66, 67].

These inversion techniques for the matter distribution in galaxy-cluster lenses have by now been applied to numerous objects [68, 69, 70]. For most of them, the mass-to-light ratios turned out to be  $M/L \simeq (250 - 300) h M_\odot/L_\odot$  in blue and  $M/L \simeq (150 - 200) h M_\odot/L_\odot$  in red light, respectively [see 71, 72, 73, for some examples]. Similar to weak lensing by galaxies, the masses quoted here are typically derived from parameterised density profiles adapted to the measured lensing signal and integrated to a fixed radius of order  $1 h^{-1} \text{ Mpc}$ . Statistically combining the weak-lensing signal of galaxy groups, the mass range in which mass-to-light ratios can be probed could be extended towards lower masses. For galaxy groups with masses around  $(10^{13} - 10^{14}) M_\odot$ , values of  $M/L \simeq 180 h M_\odot/L_\odot$  in blue and  $M/L \simeq 250 h M_\odot/L_\odot$  in red spectral ranges have been obtained [74, 75].

By a similar statistical analysis of gravitational lensing together with the optical light distribution, the mass-to-light ratio of the central brightest galaxies in galaxy clusters was found to be  $M/L \simeq 360 h M_\odot/L_\odot$  [76, 77]. Mass and light generally appear well correlated in weakly lensing clusters. Contradicting claims from individual objects could not be confirmed [78, 79]. A very peculiar case is the galaxy cluster Abell 2744, whose galaxies and dark matter are displaced from the X-ray emission [80], see Fig. 4.

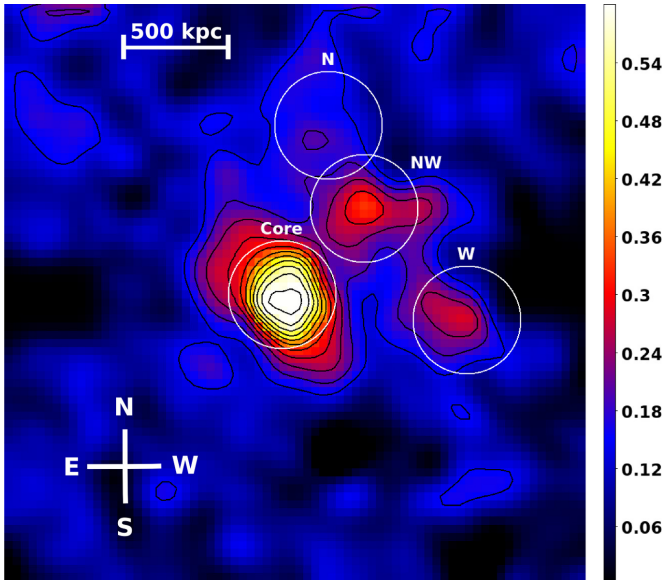


Figure 4: Mass map of the galaxy cluster Abell 2744 (sometimes called “Pandora’s box”), reconstructed from the weak-lensing signal [reprinted with permission from 80, Fig. 3]. At least two, maybe three galaxy clusters have collided here. The colour encodes the convergence  $\kappa$ .

### 7.3 Lensing and X-ray emission

Comparing the surface-brightness distribution of the X-rays emitted by the hot intracluster medium with the surface-density contours obtained from weak lensing, interesting phenomena are uncovered. While the X-ray surface brightness follows the matter density in many clusters (see [81, 82, 83, 84] for examples), instructive deviations have been discovered.

Generally, deviations between the morphologies of the surface-mass density and the X-ray surface brightness are attributed to dynamical processes going on in galaxy clusters which are merging with other clusters or are otherwise out of equilibrium. In merging clusters, the X-ray gas is typically found lagging behind the dark matter, as expected for hot gas embedded into collision-less dark-matter halos [85, 86, 87, 88].

A particularly interesting case is the cluster 1E 0657–558, called the bullet cluster, whose X-ray emission appears in between two galaxy concentrations and dark-matter distributions recovered from weak lensing [89, 90, 91]. The morphology of the bullet cluster suggests that two clusters have lost their gas by friction while passing each other in the course of a merger. Other clusters showing similar morphology have since been found [92].

If the hypothetical dark-matter particles interacted with each other, such a separation between gas and dark matter would be suppressed. Thus, from gas lagging behind the dark matter in merging clusters, and from small dark-matter core radii, limits could be obtained for the self-interaction cross section of the dark-matter particles, typically finding values  $\lesssim (0.1 - 1) \text{ cm}^2 \text{ g}^{-1}$ , comparable to values derived from strong gravitational lensing by clusters [93, 94, 95, 87, 96].

Apart from gravitational lensing, masses of galaxy clusters can be estimated from the X-ray emission and the kinematics of the cluster galaxies. Although different mass estimates agree well in some clusters (e.g. [84, 97, 98, 88, 99, 100, 101, 68, 102, 103]), substantial discrepancies are often found and interpreted

as signalling dynamical processes in unrelaxed cluster cores or systematics in the data interpretation [104, 105, 106, 107, 108, 109, 110, 111]. Signs of dynamical activity are often seen in massive galaxy clusters, while less massive, cooler clusters seem to be closer to equilibrium [112, 113, 114, 115].

Even though galaxy clusters are the population of cosmic objects forming last in cosmic history, spectacular examples of massive, distant clusters have been found. The weak-lensing signals of many distant clusters have been measured, typically confirming the presence of well-developed, massive and compact clusters at that epoch [116, 71, 81, 117, 99, 118], but also frequently indicating violent dynamical activity in cluster cores [83, 106, 88, 119].

### 7.4 Cluster density profiles

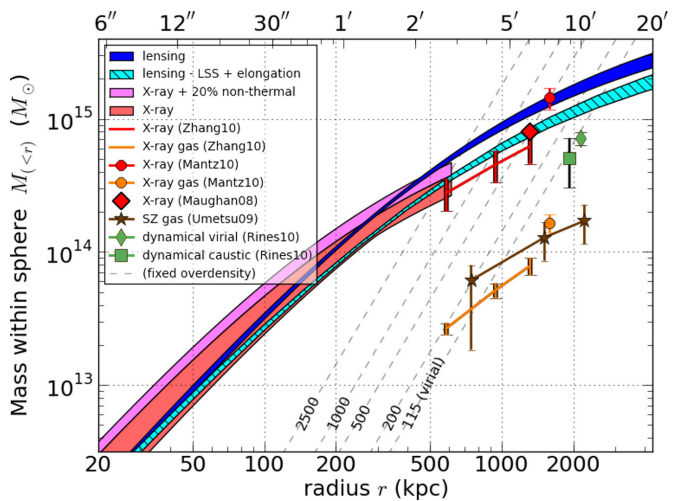


Figure 5: Radial mass profiles of the galaxy cluster Abell 2261, obtained from gravitational lensing and from different types of data [reprinted with permission from 120, Fig. 13].

The radial matter-density profile in galaxy clusters is fundamentally important for cosmology because numerical simulations routinely show that a near-universal density profile is expected,

$$\rho(x) = \frac{\rho_s}{x(1+x)^2}, \quad x := \frac{r}{r_s}. \quad (61)$$

It is called *NFW profile* after Navarro, Frenk and White who first described it [121, 122]. While first studies found that cluster mass-density profiles could be well fit by an isothermal profile (falling off in projection with radius  $r$  as  $r^{-1}$ ) or equally well by NFW and isothermal profiles [82, 123, 124, 105], the NFW profile became preferred as the data quality improved [123, 42, 125].

In addition to its density parameter  $\rho_s$ , the NFW profile is characterised by a scale radius  $r_s$ . Simulations find that the ratio between the overall (virial) radius and the scale radius, called concentration, is gently decreasing with mass. While cluster profiles derived from weak gravitational lensing alone tend to have somewhat larger scale radii than expected, possibly reflecting deviations from spherical symmetry [82, 84, 72, 88, 45], scale radii well in the expected range are typically derived from data of high quality analysed with sophisticated methods [123, 94, 126]. An exciting step beyond determining density profiles is the measurement of the subhalo mass function in the Coma galaxy cluster [127].

The large-scale matter distribution in front of and behind galaxy clusters is projected onto them and can affect weak-lensing mass determinations. Estimates based on simulations and analytic calculations indicate that cluster mass estimates from weak gravitational lensing can be changed at the level of up to 40 per cent, and that uncertainties of the total mass estimates can be approximately doubled by projection. Cluster density profiles, however, should only be weakly affected [128, 129, 130, 86].

## 7.5 Cluster detection

Several detections of clusters with very high mass-to-light ratios have been claimed and raised the question whether cluster-sized dark-matter halos may exist which are so inefficient in producing stellar or X-ray emission that they are invisible to anything but gravitational lensing [59, 131, 132, 133, 134, 135]. The most prominent cases discussed of potentially dark clusters so far, however, did not outlast later re-analyses of the data or analyses of new data [78, 136, 79].

Weak gravitational lensing also provides a powerful way to detect galaxy clusters regardless of their directly observable signatures. Methods developed for this purpose use weighted integrals over circular apertures of the gravitational shear signal tangentially oriented with respect to the aperture centre. Numerical simulations show that these methods are highly efficient in finding suitably massive matter concentrations if parameters and weight functions are optimally chosen to carefully balance the completeness against the frequency of spurious detections [137, 138, 139, 140, 141]. Substantial samples of galaxy clusters have been routinely detected and confirmed by this technique. Their statistical analysis is likely to provide important information on the origin and evolution of non-linear cosmic structures in the near future [142, 143, 144, 145, 146, 147, 148, 149, 150, 151, 152, 153, 154, 155, 156, 157, 158, 159]. Sufficiently numerous and well-defined cluster samples may well be the most sensitive probe into a possible time dependence of the enigmatic dark energy supposed to drive our Universe apart in an accelerated fashion [132, 133, 160, 161, 162, 163, 164, 165].

Galaxy clusters are embedded into a network of filamentary structures [166, 167, 168, 169] which may be traced by direct mapping or with linear filtering techniques similar to those developed for halo detection, albeit with generally low signal-to-noise ratio [170, 171, 172, 173].

## 8 Weak gravitational lensing by large-scale structures

### 8.1 Expectations and measurements

Weak gravitational lensing by large-scale structures, or cosmological weak lensing, is a rich and rapidly developing field which is covered in detail by several dedicated reviews [13, 14, 174, 175, 15, 176, 177]. We summarise the most important aspects here and refer the interested reader to those reviews for further detail.

Early studies used analytic calculations to show that the standard deviation of image ellipticities induced by cosmological weak lensing were of order a few per cent on arc-minute angular scales. A first attempt at measuring this tiny signal

placed an upper limit in agreement with theoretical expectations [178, 179, 180, 181]. Since weak cosmological lensing depends sensitively on the non-linear evolution of the large-scale structures, numerical simulations are required for precisely estimating the expected amplitude of the signal and the shape of the ellipticity correlation function [182, 183, 184, 185, 186, 187]. The cosmological potential of large weak-lensing surveys was quickly pointed out [188, 189, 190], emphasising the possibility of measuring in particular the matter density parameter  $\Omega_{m0}$  and the amplitude  $\sigma_8$  of the dark-matter power spectrum.

The first detections of cosmological weak lensing were announced around the turn of the century [191, 192, 193, 194, 195]. Given the enormous difficulty of the measurement and the different telescopes, cameras, and analysis techniques used, the agreement between these results and their compatibility with theoretical expectations was surprising and encouraging at the same time.

Assuming a spatially flat cosmological model, the cosmological parameters  $\Omega_{m0}$  and  $\sigma_8$  were derived from measurements of the cosmic-shear correlation function. Since these parameters are degenerate, higher than two-point statistics are needed for constraining them separately [196, 197, 198, 199]. Enormous effort was subsequently devoted to calibrating weak-lensing measurements, to designing optimal cosmic-shear estimators and studying their noise properties, and to shaping theoretical expectations [200, 201, 202, 203, 204, 205, 206].

Numerous weak-lensing surveys have meanwhile been conducted, and cosmological parameters derived from them. Values obtained for the matter-fluctuation amplitude  $\sigma_8$  at fixed  $\Omega_{m0} = 0.3$  tend to agree within the error bars, but the scatter is still substantial: They fall into the range 0.65 – 1.06, with much of the uncertainty due to remaining systematics in the data analysis [195, 207, 208, 209, 210, 211, 212, 213, 214, 215, 216, 217, 218, 219, 220, 221, 222, 223, 206].

Dedicated weak-lensing surveys of increasing portions of the sky have been concluded with remarkable success, are ongoing or being planned, with the solid angles covered by the surveys increasing in steps of a factor of ten. The Canada-France-Hawaii Telescope Lensing Survey (CFHTLenS) has covered 154 square degrees [224, 225]; see Figs. 6 and 7 for selected results. The Kilo-Degree Survey [226] and the Dark-Energy Survey [227] are covering 1500 and 5000 square degrees, respectively. The Large Synoptic Survey Telescope and the Euclid satellite are planned to cover approximately 15000 square degrees [228, 229]. Besides mapping dark matter and determining cosmological parameters, a primary goal of these surveys is to constrain the growth of cosmological structures and thereby the nature of the dark energy. Future wide-field radio surveys will also offer exciting possibilities for cosmological applications of weak gravitational lensing [230, 231, 232].

### 8.2 Systematics

Numerical simulations show that the Born approximation is valid to a very high degree [235, 236, 187]. As shown above, the gravitational lensing effects even by widely extended lenses can be summarised by a scalar potential. Thus, weak lensing can only cause such distortion patterns which can be described by derivatives of a scalar potential. This motivates the decomposition of distortion patterns in gradient and curl contributions, termed *E* and *B* modes in analogy to electrodynamics. Significant *B* modes in the data are interpreted as

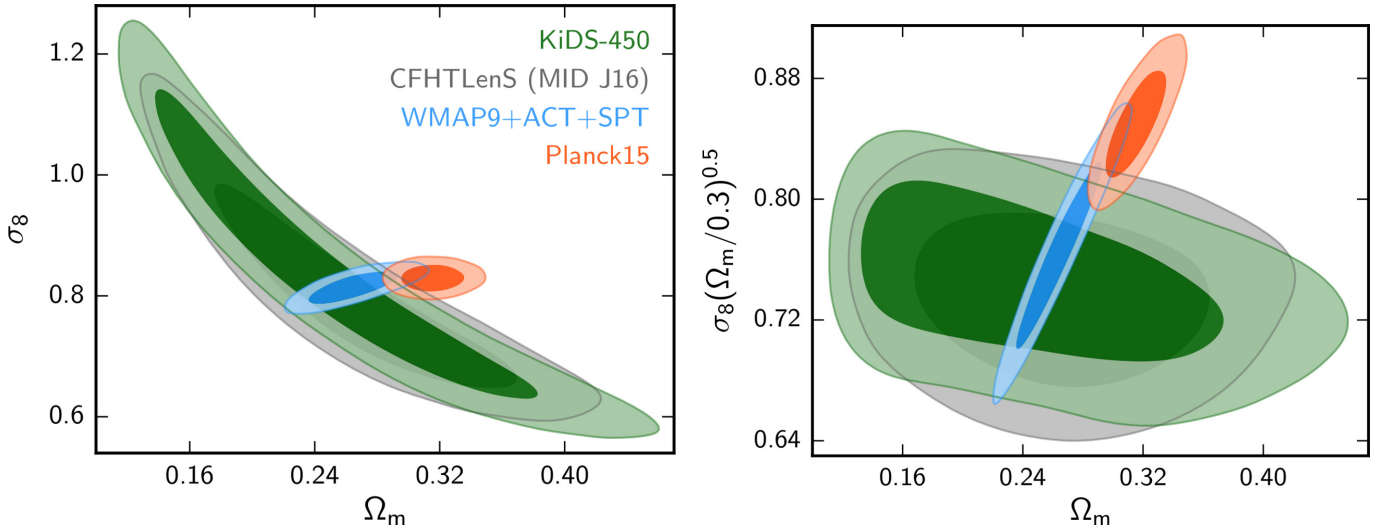


Figure 6: Constraints on two cosmological parameters, the normalisation parameter  $\sigma_8$  and the matter-density parameter  $\Omega_{m0}$ , obtained from cosmic-shear correlation functions measured from  $\sim 450$  square degrees of the KiDS survey [reprinted with permission from 233, Fig. 6]. The green area in the panel shows constraints from the KiDS survey, the grey area those from the CFHTLenS survey [234]. In the right panel, the vertical axis shows the combined parameter  $\sigma_8(\Omega_{m0}/0.3)^{0.5}$  that weak cosmological lensing is sensitive to. Blue and red areas show the independent constraints from CMB measurements prior to Planck and by Planck, respectively.

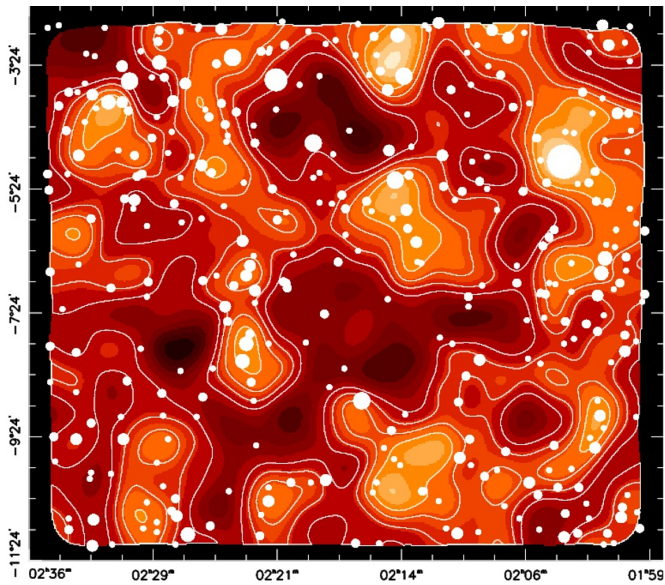


Figure 7: Map of matter distribution in one of the CFHTLenS fields, reconstructed from weak gravitational lensing [225, Fig. 8]. The white dots mark positions of local galaxy concentrations.

remainders of undetected or incompletely removed systematics. More or less significant  $B$  modes have been found in almost all weak-lensing surveys. Meticulous studies revealed that they originated from various effects, among them incomplete correction of astigmatism in the telescope optics, source clustering or finite-field effects. Once these reasons had been identified, methods were developed for removing the  $B$  modes they caused [237, 238, 215, 239, 240, 241].

At least five important sources of systematic error plague weak-lensing measurements: astigmatism of the telescope optics, miscalibrated distortion measurements, insufficient knowledge of the non-linear density-fluctuation power spec-

trum, insufficient information on the distance distribution of the lensed galaxies, and intrinsic alignments of background sources. All these effects have been addressed in detail, and sophisticated techniques have been developed for removing them from the data or at least for quantifying them [242, 18, 243, 244, 245, 19, 20, 187, 246, 247]. By now, the largest sources of systematic error are probably the distances of the background sources, the non-linear evolution of the power spectrum and the influence of baryonic matter on the dark-matter distribution.

The potentially harmful effect of intrinsic rather than lensing-induced galaxy alignments depends obviously on the depth of the survey. Deep surveys project galaxy images along light paths which are substantially longer than any large-scale structure correlation scale and thus suppress any spurious signal due to intrinsic alignments of physically neighbouring galaxies. In shallow surveys, however, intrinsic source alignments may substantially contaminate any weak-shear signal. The degree to which intrinsic alignments affect weak-lensing measurements is still a matter of lively debate in both theory and observation, and between both disciplines [248, 249, 250, 251, 252, 253, 254, 255, 256, 257, 258, 259, 260, 261, 234, 262, 263, 264, 265, 266, 267, 268, 269].

Likewise, possibilities for removing the signal contamination due to intrinsic alignments are being discussed extensively. They advocate using approximate photometric distance information to remove physically close pairs of source galaxies from the analysis. Applications of this technique suggest that the effects of intrinsic alignments should be near the lower end of the theoretical predictions. Foreground galaxies are additionally aligned with the large-scale structures lensing the background galaxies, thus giving rise to an indirect alignment between galaxies at different redshifts. This further effect can substantially reduce the measured shear signal, leading to a likely underestimate of the  $\sigma_8$  parameter by several per cent [270, 209, 271, 272, 273, 274, 275].

### 8.3 Perspectives

Approximately since the turn of the century, cosmology has a standard model, most of whose parameters are now known at the per-cent level or better. To a large degree, this was enabled by the precise measurements of the temperature and polarisation fluctuations in the CMB, combined with surveys of the large-scale galaxy distribution and measurements of the cosmic expansion rate by means of type-Ia supernovae. What is the role of weak gravitational lensing in this context?

Cosmological parameter constraints from the CMB alone suffer from degeneracies which can only be broken using additional information. By measuring the dark-matter density and the normalisation of its fluctuation amplitude directly, gravitational lensing adds constraints which substantially narrow the parameter ranges allowed by the CMB alone [276, 277, 278]. Also, the exploitation of higher than two-point statistics helps in breaking degeneracies in the weak-lensing parameter estimates and in analysing deviations from the primordial Gaussian statistics that develop from non-linear structure growth [279, 280, 281].

Perhaps the most exciting promise of weak gravitational lensing by large-scale structures derives from its potential to study the three-dimensional distribution of dark structures, originating from the distance dependence of the lensing observables. Although these observables measure the tidal field of the two-dimensional, projected matter distribution, selecting sources at multiple distances allows structures along the line-of-sight to be resolved. The distances to the source galaxies can be estimated with sufficient accuracy by photometric (rather than spectroscopic) methods. Such estimates can be used to group the source-galaxy population by distance shells and thus to extract three-dimensional information on the lensing matter distribution [282, 283, 284, 285, 286, 225, 287].

Even poorly resolved three-dimensional information from weak gravitational lensing constrains the growth of cosmic structures along the line-of-sight from the distant and past universe until the present. Sufficiently precise measurements of weak lensing in wide fields on the sky should thus enable accurate constraints on the dynamics of the accelerated expansion of the Universe. This constitutes the strongest motivation for weak-lensing surveys on increasing areas and from space, and for getting remaining systematics under ever better control [288, 289, 290, 291, 292, 293, 294, 295, 296, 297, 298, 299, 300]. A further exciting perspective for gravitational-lensing research is the possibility to test the theory of gravity itself [301, 302, 303, 304].

### 8.4 Cosmic magnification

Gravitational lensing not only distorts the images of distant galaxies, but also magnifies them. As shown above to linear order, the power spectrum of the magnification is just four times the power spectrum of the gravitational shear, hence both magnification and shear contain the same amount of information. The gravitational shear, however, can much more easily be measured than the magnification because the ellipticities of distant galaxies average to zero while the intrinsic flux of any given source is generally unknown.

Currently the most promising method for detecting gravitational magnification rests on the so-called magnification bias. If a population of distant sources is observed within a certain

solid angle  $\delta\Omega$  on the sky where the magnification is  $\mu$ , fainter sources become visible there. At the same time, their number density is reduced because the solid angle is enlarged by the magnification. The net effect depends on how many more sources the magnification lifts above the sensitivity threshold of the observation. If the number of visible sources increases more than linearly with the magnification, the dilution by the enlarged solid angle is outweighed and the magnification causes more sources to become visible.

There is a class of intrinsically bright sources in the distant universe, the so-called quasi-stellar objects or QSOs, which appear more numerous on magnified areas of the sky. At the same time, the large-scale structures responsible for gravitational lensing contain more galaxies where the matter is more concentrated. This correlation of galaxies with the magnifying lenses, together with the increase of QSO number counts due to the lensing magnification, creates a measurable, apparent correlation between distant QSOs and foreground galaxies. Due to the non-linearity of the magnification in the convergence and the shear, accurate theoretical predictions for cosmic magnification are more difficult than for cosmic shear. Typical magnifications are of order 10 per cent for moderately distant sources. In addition to QSOs, certain populations of distant galaxies can also be used as sources [305, 306, 307, 308, 309, 310, 311, 312, 313].

The existence of correlations between distant QSOs and foreground galaxies could quickly be established [314, 315, 316, 317, 318, 319, 320]. It was considerably more difficult to determine accurate expected amplitudes and angular scales of these correlations and finally converge on results that could be understood theoretically, including systematic effects due to extinction by intervening dust and fluctuations in the correlation between the foreground galaxies and the gravitationally-lensing large-scale structures [321, 322, 323, 324, 325, 326, 327, 328, 329, 330].

The weakness of the signal and the interference of a variety of confusing effects required large surveys taken in several photometric bands to unambiguously detect cosmic magnification and to extract cosmological information from it, but the information gain is expected to be substantial [331, 332, 333, 334, 335, 336, 337, 338, 339, 340, 341, 342, 343, 344].

### 8.5 Gravitational lensing of the CMB

The effects of gravitational lensing on the CMB are rich in detail [28]. Pioneering studies showed that the CMB is expected to be measurably lensed by cosmic structures in a way which resembles a diffusion process and builds up small-scale structure at the same time [345, 346, 347, 348, 349, 350, 351, 352, 353, 354]. As mentioned above, gravitational lensing of the CMB can be identified by the coupling lensing creates between different Fourier modes of the temperature-fluctuation pattern in the CMB [355, 356, 357, 358, 359, 360, 361, 362, 363].

Accurate constraints of cosmological parameters from well-resolved CMB temperature fluctuations are possible only if the weak gravitational lensing effects can be quantified and corrected. At the same time, the gravitational lensing signal contained in the CMB itself can be used to break parameter degeneracies in the purely primordial CMB data [364, 365, 366, 367, 368]. After indirect evidence had been found for gravitational lensing of the CMB [369, 370], the direct and unambiguous detection of cosmological weak lensing in the CMB data was among the most fascinating results of the Planck

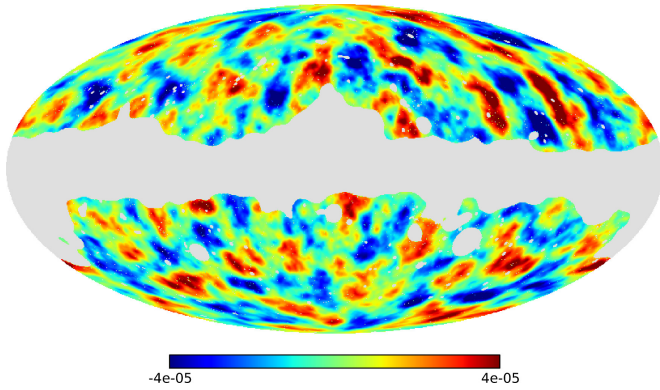


Figure 8: Sky map of the gravitational-lensing potential reconstructed from the CMB temperature fluctuations as measured by the Planck satellite [reprinted with permission from 29, Fig. 2].

satellite mission [371, 29, 372].

## 9 Summary

Gravitational lensing has two major advantages that turn it into one of the most versatile, contemporary cosmological tools: its foundation in the theory of gravity is reasonably straightforward, and it is sensitive to matter (and energy) inhomogeneities regardless of their internal physical state. Under the assumptions that gravitational lenses are weak, move slowly with respect to the cosmological rest frame, and are much smaller than cosmological length scales, the effects of gravitational lensing are entirely captured by a two-dimensional effective lensing potential. The Hessian matrix of this potential defines the local imaging properties of gravitational lenses. The Poisson equation, relating the Laplacian of the potential to the surface-mass density, allows one to infer the lensing matter distribution from observable image distortions.

Weak gravitational lensing has been applied on a broad range of scales. Weak lensing of galaxies by galaxies was used to infer mass-to-light ratios of galaxies, their sizes, and constraints on their radial density profiles. Besides constraining the density profile and the mass-to-light ratio, weak lensing by galaxy clusters has allowed us to map the spatial distribution of dark and luminous matter in clusters as well as to constrain the amount of substructure in them. In spectacular examples, it was possible to show that dark and luminous matter must have been separated in cluster collisions, yielding tight upper limits on the self-interaction cross section of the hypothetical dark-matter particles. On yet larger scales, cosmological weak lensing is now routinely being used to constrain the amount of dark matter and the amplitude of its fluctuations, and also to map the matter distribution in wide fields on the sky. Finally, it has recently become possible to measure the cosmological weak lensing effect on temperature fluctuations in the CMB and to create sky maps of what could be called the index of refraction of the entire visible universe.

## Acknowledgements

This work was supported in part by the Transregional Collaborative Research Centre TR 33 “The Dark Universe” of the

German Science Foundation (DFG). We are grateful to Olivier Minazzoli for inviting us to write this contribution to Scholarpedia and for his patience with our very slow return. We also wish to thank the many colleagues who helped us shape our views on weak lensing with enlightening and enjoyable discussions, way too many to name them all individually – they form a good fraction of the authors cited below! (Unfortunately not including Sir Isaac Newton.)

## References

- [1] Sir I. Newton. *Opticks: or, A treatise of the reflexions, refractions, inflexions and colours of light*. Sam. Smith and Benj. Walford, 1704.
- [2] J. G. von Soldner. *Ueber die Ablenkung eines Lichtstrals von seiner geradlinigen Bewegung, durch die Attraktion eines Weltkörpers, an welchem er nahe vorbei geht*, pages 161–172. G. A. Lange, 1804.
- [3] A. Einstein. Über den Einfluß der Schwerkraft auf die Ausbreitung des Lichtes. *Annalen der Physik*, 340:898–908, 1911. doi: 10.1002/andp.19113401005.
- [4] A. Einstein. Die Grundlage der allgemeinen Relativitätstheorie. *Annalen der Physik*, 354:769–822, 1916. doi: 10.1002/andp.19163540702.
- [5] A. S. Eddington. The total eclipse of 1919 May 29 and the influence of gravitation on light. *The Observatory*, 42:119–122, March 1919.
- [6] A. Einstein. Prüfung der allgemeinen Relativitätstheorie. *Naturwissenschaften*, 7:776–776, October 1919. doi: 10.1007/BF01489445.
- [7] A. Einstein. Lens-Like Action of a Star by the Deviation of Light in the Gravitational Field. *Science*, 84:506–507, December 1936. doi: 10.1126/science.84.2188.506.
- [8] F. Zwicky. Nebulae as Gravitational Lenses. *Physical Review*, 51: 290–290, February 1937. doi: 10.1103/PhysRev.51.290.
- [9] F. Zwicky. Die Rotverschiebung von extragalaktischen Nebeln. *Helvetica Physica Acta*, 6:110–127, 1933.
- [10] D. Walsh, R. F. Carswell, and R. J. Weymann. 0957 + 561 A, B - Twin quasistellar objects or gravitational lens. *Nat*, 279:381–384, May 1979. doi: 10.1038/279381a0.
- [11] P. Schneider, J. Ehlers, and E. E. Falco. *Gravitational Lenses*. Springer, 1992.
- [12] R. Narayan and M. Bartelmann. Gravitational lensing. In A. Dekel & J. P. Ostriker, editor, *Formation of Structure in the Universe*, pages 360–+, 1999.
- [13] Y. Mellier. Probing the Universe with Weak Lensing. *ARA&A*, 37: 127–189, 1999.
- [14] M. Bartelmann and P. Schneider. Weak gravitational lensing. *Phys. Rep.*, 340:291–472, January 2001.
- [15] A. Refregier. Weak Gravitational Lensing by Large-Scale Structure. *ARA&A*, 41:645–668, 2003.
- [16] G. Meylan, P. Jetzer, P. North, P. Schneider, C. S. Kochanek, and J. Wambsganss, editors. *Gravitational Lensing: Strong, Weak and Micro*, 2006.
- [17] M. Bartelmann. TOPICAL REVIEW Gravitational lensing. *Classical and Quantum Gravity*, 27(23):233001, December 2010. doi: 10.1088/0264-9381/27/23/233001.
- [18] C. Heymans, L. Van Waerbeke, D. Bacon, J. Berge, G. Bernstein, E. Bertin, S. Bridle, M. L. Brown, D. Clowe, H. Dahle, T. Erben, M. Gray, M. Hettterscheidt, H. Hoekstra, P. Hudelot, M. Jarvis, K. Kuijken, V. Margoniner, R. Massey, Y. Mellier, R. Nakajima, A. Refregier, J. Rhodes, T. Schrabback, and D. Wittman. The Shear Testing Programme - I. Weak lensing analysis of simulated ground-based observations. *MNRAS*, 368:1323–1339, May 2006. doi: 10.1111/j.1365-2966.2006.10198.x.

- [19] R. Massey, C. Heymans, J. Bergé, G. Bernstein, S. Bridle, D. Clowe, H. Dahle, R. Ellis, T. Erben, M. Hetterscheidt, F. W. High, C. Hirata, H. Hoekstra, P. Hudelot, M. Jarvis, D. Johnston, K. Kuijken, V. Margoniner, R. Mandelbaum, Y. Mellier, R. Nakajima, S. Paulin-Henriksson, M. Peebles, C. Roat, A. Refregier, J. Rhodes, T. Schrabback, M. Schirmer, U. Seljak, E. Semboloni, and L. van Waerbeke. The Shear Testing Programme 2: Factors affecting high-precision weak-lensing analyses. *MNRAS*, 376:13–38, March 2007. doi: 10.1111/j.1365-2966.2006.11315.x.
- [20] S. Bridle, S. T. Balan, M. Bethge, M. Gentile, S. Harmeling, C. Heymans, M. Hirsch, R. Hosseini, M. Jarvis, D. Kirk, T. Kitching, K. Kuijken, A. Lewis, S. Paulin-Henriksson, B. Schölkopf, M. Velander, L. Voigt, D. Witherick, A. Amara, G. Bernstein, F. Courbin, M. Gill, A. Heavens, R. Mandelbaum, R. Massey, B. Moghaddam, A. Rassat, A. Réfrégier, J. Rhodes, T. Schrabback, J. Shawe-Taylor, M. Shmakova, L. van Waerbeke, and D. Wittman. Results of the GREAT08 Challenge: an image analysis competition for cosmological lensing. *MNRAS*, 405:2044–2061, July 2010. doi: 10.1111/j.1365-2966.2010.16598.x.
- [21] P. Melchior, R. Andrae, M. Maturi, and M. Bartelmann. Deconvolution with shapelets. *A&A*, 493:727–734, January 2009. doi: 10.1051/0004-6361:200810472.
- [22] P. Melchior, M. Viola, B. M. Schäfer, and M. Bartelmann. Weak gravitational lensing with DEIMOS. *MNRAS*, 412:1552–1558, April 2011. doi: 10.1111/j.1365-2966.2010.17875.x.
- [23] P. Melchior and M. Viola. Means of confusion: how pixel noise affects shear estimates for weak gravitational lensing. *MNRAS*, 424:2757–2769, August 2012. doi: 10.1111/j.1365-2966.2012.21381.x.
- [24] A. Refregier, T. Kacprzak, A. Amara, S. Bridle, and B. Rowe. Noise bias in weak lensing shape measurements. *MNRAS*, 425:1951–1957, September 2012. doi: 10.1111/j.1365-2966.2012.21483.x.
- [25] M. Viola, P. Melchior, and M. Bartelmann. Shear-flexion cross-talk in weak-lensing measurements. *MNRAS*, 419:2215–2225, January 2012. doi: 10.1111/j.1365-2966.2011.19872.x.
- [26] R. Massey, H. Hoekstra, T. Kitching, J. Rhodes, M. Cropper, J. Amiaux, D. Harvey, Y. Mellier, M. Meneghetti, L. Miller, S. Paulin-Henriksson, S. Pires, R. Scaramella, and T. Schrabback. Origins of weak lensing systematics, and requirements on future instrumentation (or knowledge of instrumentation). *MNRAS*, 429:661–678, February 2013. doi: 10.1093/mnras/sts371.
- [27] L. Miller, C. Heymans, T. D. Kitching, L. van Waerbeke, T. Erben, H. Hildebrandt, H. Hoekstra, Y. Mellier, B. T. P. Rowe, J. Coupon, J. P. Dietrich, L. Fu, J. Harnois-Déraps, M. J. Hudson, M. Kilbinger, K. Kuijken, T. Schrabback, E. Semboloni, S. Vafaei, and M. Velander. Bayesian galaxy shape measurement for weak lensing surveys - III. Application to the Canada-France-Hawaii Telescope Lensing Survey. *MNRAS*, 429:2858–2880, March 2013. doi: 10.1093/mnras/sts454.
- [28] A. Lewis and A. Challinor. Weak gravitational lensing of the CMB. *Phys. Rep.*, 429:1–65, June 2006. doi: 10.1016/j.physrep.2006.03.002.
- [29] Planck Collaboration, P. A. R. Ade, N. Aghanim, M. Arnaud, M. Ashdown, J. Aumont, C. Baccigalupi, A. J. Banday, R. B. Barreiro, J. G. Bartlett, and et al. Planck 2015 results. XV. Gravitational lensing. *A&A*, 594:A15, September 2016. doi: 10.1051/0004-6361/201525941.
- [30] T. G. Brainerd, R. D. Blandford, and I. Smail. Weak Gravitational Lensing by Galaxies. *ApJ*, 466:623–+, August 1996.
- [31] T. Treu. Strong Lensing by Galaxies. *ARA&A*, 48:87–125, September 2010. doi: 10.1146/annurev-astro-081309-130924.
- [32] I. P. dell’Antonio and J. A. Tyson. Galaxy Dark Matter: Galaxy-Galaxy Lensing in the Hubble Deep Field. *ApJL*, 473:L17+, December 1996.
- [33] P. Schneider and H. Rix. Quantitative Analysis of Galaxy-Galaxy Lensing. *ApJ*, 474:25–+, January 1997.
- [34] P. Natarajan and J. Kneib. Lensing by galaxy haloes in clusters of galaxies. *MNRAS*, 287:833–847, June 1997.
- [35] B. Geiger and P. Schneider. Constraining the mass distribution of cluster galaxies by weak lensing. *MNRAS*, 295:497–+, April 1998.
- [36] B. Geiger and P. Schneider. A simultaneous maximum likelihood approach for galaxy-galaxy lensing and cluster lens reconstruction. *MNRAS*, 302:118–130, January 1999.
- [37] P. Natarajan, J. Kneib, and I. Smail. Evidence for Tidal Stripping of Dark Matter Halos in Massive Cluster Lenses. *ApJL*, 580:L11–L15, November 2002.
- [38] H. Hoekstra, H. K. C. Yee, and M. D. Gladders. Properties of Galaxy Dark Matter Halos from Weak Lensing. *ApJ*, 606:67–77, May 2004.
- [39] P. Fischer, T. A. McKay, E. Sheldon, A. Connolly, A. Stebbins, J. A. Frieman, B. Jain, M. Joffe, D. Johnston, G. Bernstein, J. Annis, N. A. Bahcall, J. Brinkmann, M. A. Carr, I. Csabai, J. E. Gunn, G. S. Hennesy, R. B. Hindsley, C. Hull, Ž. Ivezić, G. R. Knapp, S. Limmongkol, R. H. Lupton, J. A. Munn, T. Nash, H. J. Newberg, R. Owen, J. R. Pier, C. M. Rockosi, D. P. Schneider, J. A. Smith, C. Stoughton, A. S. Szalay, G. P. Szokoly, A. R. Thakar, M. S. Vogeley, P. Waddell, D. H. Weinberg, D. G. York, and The SDSS Collaboration. Weak Lensing with Sloan Digital Sky Survey Commissioning Data: The Galaxy-Mass Correlation Function to  $1 H^{-1}$  Mpc. *AJ*, 120:1198–1208, September 2000.
- [40] D. R. Smith, G. M. Bernstein, P. Fischer, and M. Jarvis. Weak-Lensing Determination of the Mass in Galaxy Halos. *ApJ*, 551:643–650, April 2001.
- [41] G. Wilson, N. Kaiser, G. A. Luppino, and L. L. Cowie. Galaxy Halo Masses from Galaxy-Galaxy Lensing. *ApJ*, 555:572–584, July 2001.
- [42] R. Mandelbaum, U. Seljak, R. J. Cool, M. Blanton, C. M. Hirata, and J. Brinkmann. Density profiles of galaxy groups and clusters from SDSS galaxy-galaxy weak lensing. *MNRAS*, 372:758–776, October 2006. doi: 10.1111/j.1365-2966.2006.10906.x.
- [43] L. C. Parker, H. Hoekstra, M. J. Hudson, L. van Waerbeke, and Y. Mellier. The Masses and Shapes of Dark Matter Halos from Galaxy-Galaxy Lensing in the CFHT Legacy Survey. *ApJ*, 669:21–31, November 2007. doi: 10.1086/521541.
- [44] R. Gavazzi, T. Treu, J. D. Rhodes, L. V. E. Koopmans, A. S. Bolton, S. Burles, R. J. Massey, and L. A. Moustakas. The Sloan Lens ACS Survey. IV. The Mass Density Profile of Early-Type Galaxies out to 100 Effective Radii. *ApJ*, 667:176–190, September 2007. doi: 10.1086/519237.
- [45] R. Mandelbaum, U. Seljak, and C. M. Hirata. A halo mass-concentration relation from weak lensing. *Journal of Cosmology and Astro-Particle Physics*, 8:6–+, August 2008. doi: 10.1088/1475-7516/2008/08/006.
- [46] J. Guzik and U. Seljak. Virial masses of galactic haloes from galaxy-galaxy lensing: theoretical modelling and application to Sloan Digital Sky Survey data. *MNRAS*, 335:311–324, September 2002.
- [47] U. Seljak. Constraints on galaxy halo profiles from galaxy-galaxy lensing and Tully-Fisher/Fundamental Plane relations. *MNRAS*, 334:797–804, August 2002.
- [48] H. Hoekstra, H. K. C. Yee, and M. D. Gladders. Measurement of the Bias Parameter from Weak Lensing. *ApJL*, 558:L11–L14, September 2001.
- [49] H. Hoekstra, L. van Waerbeke, M. D. Gladders, Y. Mellier, and H. K. C. Yee. Weak Lensing Study of Galaxy Biasing. *ApJ*, 577:604–614, October 2002.
- [50] X. H. Yang, H. J. Mo, G. Kauffmann, and Y. Q. Chu. Understanding the results of galaxy-galaxy lensing using galaxy-mass correlation in numerical simulations. *MNRAS*, 339:387–396, February 2003.
- [51] C. M. Hirata, R. Mandelbaum, U. Seljak, J. Guzik, N. Padmanabhan, C. Blake, J. Brinkmann, T. Budavári, A. Connolly, I. Csabai, R. Scranton, and A. S. Szalay. Galaxy-galaxy weak lensing in the Sloan Digital Sky Survey: intrinsic alignments and shear calibration errors. *MNRAS*, 353:529–549, September 2004.
- [52] E. S. Sheldon, D. E. Johnston, J. A. Frieman, R. Scranton, T. A. McKay, A. J. Connolly, T. Budavári, I. Zehavi, N. A. Bahcall, J. Brinkmann, and M. Fukugita. The Galaxy-Mass Correlation Function Measured from Weak Lensing in the Sloan Digital Sky Survey. *AJ*, 127:2544–2564, May 2004.

- [53] D. H. Weinberg, R. Davé, N. Katz, and L. Hernquist. Galaxy Clustering and Galaxy Bias in a  $\Lambda$ CDM Universe. *ApJ*, 601:1–21, January 2004.
- [54] R. Mandelbaum, C. Li, G. Kauffmann, and S. D. M. White. Halo masses for optically selected and for radio-loud AGN from clustering and galaxy-galaxy lensing. *MNRAS*, 393:377–392, February 2009. doi: 10.1111/j.1365-2966.2008.14235.x.
- [55] M. Cacciato, F. C. van den Bosch, S. More, R. Li, H. J. Mo, and X. Yang. Galaxy clustering and galaxy-galaxy lensing: a promising union to constrain cosmological parameters. *MNRAS*, 394:929–946, April 2009. doi: 10.1111/j.1365-2966.2008.14362.x.
- [56] P. Simon, T. Erben, P. Schneider, C. Heymans, H. Hildebrandt, H. Hoekstra, T. D. Kitching, Y. Mellier, L. Miller, L. Van Waerbeke, C. Bonnett, J. Coupon, L. Fu, M. J. Hudson, K. Kuijken, B. T. P. Rowe, T. Schrabback, E. Semboloni, and M. Velander. CFHTLenS: higher order galaxy-mass correlations probed by galaxy-galaxy-galaxy lensing. *MNRAS*, page 710, February 2013. doi: 10.1093/mnras/stt069.
- [57] S. More, H. Miyatake, R. Mandelbaum, M. Takada, D. N. Spergel, J. R. Brownstein, and D. P. Schneider. The Weak Lensing Signal and the Clustering of BOSS Galaxies. II. Astrophysical and Cosmological Constraints. *ApJ*, 806:2, June 2015. doi: 10.1088/0004-637X/806/1/2.
- [58] N. Kaiser and G. Squires. Mapping the dark matter with weak gravitational lensing. *ApJ*, 404:441–450, February 1993.
- [59] G. Fahlman, N. Kaiser, G. Squires, and D. Woods. Dark matter in MS 1224 from distortion of background galaxies. *ApJ*, 437:56–62, December 1994.
- [60] C. Seitz and P. Schneider. Steps towards nonlinear cluster inversion through gravitational distortions II. Generalization of the Kaiser and Squires method. *A&A*, 297:287–+, May 1995.
- [61] C. Seitz and P. Schneider. Cluster lens reconstruction using only observed local data: an improved finite-field inversion technique. *A&A*, 305:383–+, January 1996.
- [62] M. Bartelmann, R. Narayan, S. Seitz, and P. Schneider. Maximum-likelihood Cluster Reconstruction. *ApJL*, 464:L115+, June 1996.
- [63] S. Seitz, P. Schneider, and M. Bartelmann. Entropy-regularized maximum-likelihood cluster mass reconstruction. *A&A*, 337:325–337, September 1998.
- [64] M. Bradač, T. Erben, P. Schneider, H. Hildebrandt, M. Lombardi, M. Schirmer, J.-M. Miralles, D. Clowe, and S. Schindler. Strong and weak lensing united. *A&A*, 437:49–60, July 2005. doi: 10.1051/0004-6361:20042234.
- [65] M. Bradač, D. Clowe, A. H. Gonzalez, P. Marshall, W. Forman, C. Jones, M. Markevitch, S. Randall, T. Schrabback, and D. Zaritsky. Strong and Weak Lensing United. III. Measuring the Mass Distribution of the Merging Galaxy Cluster IES 0657-558. *ApJ*, 652:937–947, December 2006. doi: 10.1086/508601.
- [66] M. Cacciato, M. Bartelmann, M. Meneghetti, and L. Moscardini. Combining weak and strong lensing in cluster potential reconstruction. *A&A*, 458:349–356, November 2006. doi: 10.1051/0004-6361:20054582.
- [67] J. Merten, M. Cacciato, M. Meneghetti, C. Mignone, and M. Bartelmann. Combining weak and strong cluster lensing: applications to simulations and MS 2137. *A&A*, 500:681–691, June 2009. doi: 10.1051/0004-6361/200810372.
- [68] A. von der Linden, M. T. Allen, D. E. Applegate, P. L. Kelly, S. W. Allen, H. Ebeling, P. R. Burchat, D. L. Burke, D. Donovan, R. G. Morris, R. Blandford, T. Erben, and A. Mantz. Weighing the Giants - I. Weak-lensing masses for 51 massive galaxy clusters: project overview, data analysis methods and cluster images. *MNRAS*, 439:2–27, March 2014. doi: 10.1093/mnras/stt1945.
- [69] D. E. Applegate, A. von der Linden, P. L. Kelly, M. T. Allen, S. W. Allen, P. R. Burchat, D. L. Burke, H. Ebeling, A. Mantz, and R. G. Morris. Weighing the Giants - III. Methods and measurements of accurate galaxy cluster weak-lensing masses. *MNRAS*, 439:48–72, March 2014. doi: 10.1093/mnras/stt2129.
- [70] M. Meneghetti, P. Natarajan, D. Coe, E. Contini, G. De Lucia, C. Giocoli, A. Acebron, S. Borgani, M. Bradac, J. M. Diego, A. Hoag, M. Ishigaki, T. L. Johnson, E. Jullo, R. Kawamata, D. Lam, M. Limousin, J. Liesenborgs, M. Oguri, K. Sebesta, K. Sharon, L. L. R. Williams, and A. Zitrin. The Frontier Fields Lens Modeling Comparison Project. *ArXiv e-prints*, June 2016.
- [71] D. Clowe, G. A. Luppino, N. Kaiser, J. P. Henry, and I. M. Gioia. Weak Lensing by Two Z approximately 0.8 Clusters of Galaxies. *ApJL*, 497: L61+, April 1998.
- [72] H. Hoekstra, M. Franx, K. Kuijken, and P. G. van Dokkum. HST large-field weak lensing analysis of MS 2053-04: study of the mass distribution and mass-to-light ratio of X-ray luminous clusters at  $0.22 < z < 0.83$ . *MNRAS*, 333:911–922, July 2002.
- [73] R. Gavazzi, Y. Mellier, B. Fort, J.-C. Cuillandre, and M. Dantel-Fort. Mass and light in the supercluster of galaxies MS0302+17. *A&A*, 422: 407–422, August 2004.
- [74] L. C. Parker, M. J. Hudson, R. G. Carlberg, and H. Hoekstra. Mass-to-Light Ratios of Galaxy Groups from Weak Lensing. *ApJ*, 634:806–812, December 2005. doi: 10.1086/497117.
- [75] M. Limousin, R. Cabanac, R. Gavazzi, J.-P. Kneib, V. Motta, J. Richard, K. Thanjavur, G. Foex, R. Pello, D. Crampton, C. Faure, B. Fort, E. Jullo, P. Marshall, Y. Mellier, A. More, G. Soucail, S. Suyu, M. Swinbank, J.-F. Sygnet, H. Tu, D. Valls-Gabaud, T. Verdugo, and J. Willis. A new window of exploration in the mass spectrum: strong lensing by galaxy groups in the SL2S. *A&A*, 502:445–456, August 2009. doi: 10.1051/0004-6361/200811473.
- [76] E. S. Sheldon, D. E. Johnston, M. Masjedi, T. A. McKay, M. R. Blanton, R. Scranton, R. H. Wechsler, B. P. Koester, S. M. Hansen, J. A. Frieman, and J. N. Annis. Cross-correlation Weak Lensing of SDSS Galaxy Clusters. III. Mass-to-Light Ratios. *ApJ*, 703:2232–2248, October 2009. doi: 10.1088/0004-637X/703/2/2232.
- [77] E. S. Sheldon, D. E. Johnston, R. Scranton, B. P. Koester, T. A. McKay, H. Oyaizu, C. Cunha, M. Lima, H. Lin, J. A. Frieman, R. H. Wechsler, J. Annis, R. Mandelbaum, N. A. Bahcall, and M. Fukugita. Cross-correlation Weak Lensing of SDSS Galaxy Clusters. I. Measurements. *ApJ*, 703:2217–2231, October 2009. doi: 10.1088/0004-637X/703/2/2217.
- [78] M. E. Gray, A. N. Taylor, K. Meisenheimer, S. Dye, C. Wolf, and E. Thommes. Probing the Distribution of Dark Matter in the A901/902 Supercluster with Weak Lensing. *ApJ*, 568:141–162, March 2002.
- [79] C. Heymans, M. E. Gray, C. Y. Peng, L. van Waerbeke, E. F. Bell, C. Wolf, D. Bacon, M. Balogh, F. D. Barazza, M. Barden, A. Böhm, J. A. R. Caldwell, B. Häußler, K. Jahnke, S. Jogee, E. van Kampen, K. Lane, D. H. McIntosh, K. Meisenheimer, Y. Mellier, S. F. Sánchez, A. N. Taylor, L. Wisotzki, and X. Zheng. The dark matter environment of the Abell 901/902 supercluster: a weak lensing analysis of the HST STAGES survey. *MNRAS*, 385:1431–1442, April 2008. doi: 10.1111/j.1365-2966.2008.12919.x.
- [80] J. Merten, D. Coe, R. Dupke, R. Massey, A. Zitrin, E. S. Cypriano, N. Okabe, B. Frye, F. G. Braglia, Y. Jiménez-Teja, N. Benítez, T. Broadhurst, J. Rhodes, M. Meneghetti, L. A. Moustakas, Jr. L. Sodré, J. Krick, and J. N. Bregman. Creation of cosmic structure in the complex galaxy cluster merger Abell 2744. *MNRAS*, 417:333–347, October 2011. doi: 10.1111/j.1365-2966.2011.19266.x.
- [81] I. M. Gioia, J. P. Henry, C. R. Mullis, H. Ebeling, and A. Wolter. RX J1716.6+6708: A Young Cluster at  $Z=0.81$ . *AJ*, 117:2608–2616, June 1999.
- [82] D. Clowe, G. A. Luppino, N. Kaiser, and I. M. Gioia. Weak Lensing by High-Redshift Clusters of Galaxies. I. Cluster Mass Reconstruction. *ApJ*, 539:540–560, August 2000.
- [83] H. Hoekstra, M. Franx, and K. Kuijken. Hubble Space Telescope Weak-Lensing Study of the  $z=0.83$  Cluster MS 1054-03. *ApJ*, 532:88–108, March 2000.
- [84] D. Clowe and P. Schneider. Wide field weak lensing observations of A1835 and A2204. *A&A*, 395:385–397, November 2002.



- [85] M. E. Machacek, M. W. Bautz, C. Canizares, and G. P. Garmire. Chandra Observations of Galaxy Cluster A2218. *ApJ*, 567:188–201, March 2002.
- [86] D. Clowe, G. De Lucia, and L. King. Effects of asphericity and substructure on the determination of cluster mass with weak gravitational lensing. *MNRAS*, 350:1038–1048, May 2004.
- [87] M. Markevitch, A. H. Gonzalez, D. Clowe, A. Vikhlinin, W. Forman, C. Jones, S. Murray, and W. Tucker. Direct Constraints on the Dark Matter Self-Interaction Cross Section from the Merging Galaxy Cluster 1E 0657-56. *ApJ*, 606:819–824, May 2004.
- [88] M. J. Jee, R. L. White, N. Benítez, H. C. Ford, J. P. Blakeslee, P. Rosati, R. Demarco, and G. D. Illingworth. Weak-Lensing Analysis of the  $z=0.8$  Cluster CL 0152-1357 with the Advanced Camera for Surveys. *ApJ*, 618:46–67, January 2005.
- [89] D. Clowe, A. Gonzalez, and M. Markevitch. Weak-Lensing Mass Reconstruction of the Interacting Cluster 1E 0657-558: Direct Evidence for the Existence of Dark Matter. *ApJ*, 604:596–603, April 2004. doi: 10.1086/381970.
- [90] D. Clowe, M. Bradač, A. H. Gonzalez, M. Markevitch, S. W. Randall, C. Jones, and D. Zaritsky. A Direct Empirical Proof of the Existence of Dark Matter. *ApJL*, 648:L109–L113, September 2006. doi: 10.1086/508162.
- [91] D. Clowe, S. W. Randall, and M. Markevitch. Catching a bullet: direct evidence for the existence of dark matter. *Nuclear Physics B Proceedings Supplements*, 173:28–31, November 2007. doi: 10.1016/j.nuclphysbps.2007.08.150.
- [92] M. Bradač, S. W. Allen, T. Treu, H. Ebeling, R. Massey, R. G. Morris, A. von der Linden, and D. Applegate. Revealing the Properties of Dark Matter in the Merging Cluster MACS J0025.4-1222. *ApJ*, 687:959–967, November 2008. doi: 10.1086/591246.
- [93] M. Meneghetti, N. Yoshida, M. Bartelmann, L. Moscardini, V. Springel, G. Tormen, and S. D. M. White. Giant cluster arcs as a constraint on the scattering cross-section of dark matter. *MNRAS*, 325:435–442, July 2001.
- [94] J. S. Arabadjis, M. W. Bautz, and G. P. Garmire. Chandra Observations of the Lensing Cluster EMSS 1358+6245: Implications for Self-interacting Dark Matter. *ApJ*, 572:66–78, June 2002.
- [95] P. Natarajan, A. Loeb, J. Kneib, and I. Smail. Constraints on the Collisional Nature of the Dark Matter from Gravitational Lensing in the Cluster A2218. *ApJL*, 580:L17–L20, November 2002.
- [96] S. W. Randall, M. Markevitch, D. Clowe, A. H. Gonzalez, and M. Bradač. Constraints on the Self-Interaction Cross Section of Dark Matter from Numerical Simulations of the Merging Galaxy Cluster 1E 0657-56. *ApJ*, 679:1173–1180, June 2008. doi: 10.1086/587859.
- [97] R. J. Irgens, P. B. Lilje, H. Dahle, and S. J. Maddox. Weak Gravitational Lensing by a Sample of X-Ray-luminous Clusters of Galaxies. II. Comparison with Virial Masses. *ApJ*, 579:227–235, November 2002.
- [98] S. M. Jia, Y. Chen, F. J. Lu, L. Chen, and F. Xiang. The analysis of Abell 1835 using a deprojection technique. *A&A*, 423:65–73, August 2004.
- [99] V. E. Margoniner, L. M. Lubin, D. M. Wittman, and G. K. Squires. Weak-Lensing Detection of Cl 1604+4304 at  $z=0.90$ . *AJ*, 129:20–25, January 2005.
- [100] H. Hoekstra. A comparison of weak-lensing masses and X-ray properties of galaxy clusters. *MNRAS*, 379:317–330, July 2007. doi: 10.1111/j.1365-2966.2007.11951.x.
- [101] Y.-Y. Zhang, A. Finoguenov, H. Böhringer, J.-P. Kneib, G. P. Smith, R. Kneissl, N. Okabe, and H. Dahle. LoCuSS: comparison of observed X-ray and lensing galaxy cluster scaling relations with simulations. *A&A*, 482:451–472, May 2008. doi: 10.1051/0004-6361:20079103.
- [102] A. von der Linden, A. Mantz, S. W. Allen, D. E. Applegate, P. L. Kelly, R. G. Morris, A. Wright, M. T. Allen, P. R. Burchat, D. L. Burke, D. Donovan, and H. Ebeling. Robust weak-lensing mass calibration of Planck galaxy clusters. *MNRAS*, 443:1973–1978, September 2014. doi: 10.1093/mnras/stu1423.
- [103] D. E. Applegate, A. Mantz, S. W. Allen, A. v. der Linden, R. G. Morris, S. Hilbert, P. L. Kelly, D. L. Burke, H. Ebeling, D. A. Rapetti, and R. W. Schmidt. Cosmology and astrophysics from relaxed galaxy clusters - IV. Robustly calibrating hydrostatic masses with weak lensing. *MNRAS*, 457:1522–1534, April 2016. doi: 10.1093/mnras/stw005.
- [104] A. D. Lewis, E. Ellingson, S. L. Morris, and R. G. Carlberg. X-Ray Mass Estimates at  $Z \sim 0.3$  for the Canadian Network for Observational Cosmology Cluster Sample. *ApJ*, 517:587–608, June 1999.
- [105] R. M. Athreya, Y. Mellier, L. van Waerbeke, R. Pelló, B. Fort, and M. Dantel-Fort. Weak lensing analysis of MS 1008-1224 with the VLT. *A&A*, 384:743–762, March 2002.
- [106] B. P. Holden, S. A. Stanford, G. K. Squires, P. Rosati, P. Tozzi, P. Eisenhardt, and H. Spinrad. Moderate-Temperature Clusters of Galaxies from the RDCS and the High-Redshift Luminosity-Temperature Relation. *AJ*, 124:33–45, July 2002.
- [107] G. W. Pratt, H. Böhringer, and A. Finoguenov. Further evidence for a merger in Abell 2218 from an XMM-Newton observation. *A&A*, 433:777–785, April 2005. doi: 10.1051/0004-6361:20041415.
- [108] M. Gitti, R. Piffaretti, and S. Schindler. Mass distribution in the most X-ray-luminous galaxy cluster RX J1347.5-1145 studied with XMM-Newton. *A&A*, 472:383–394, September 2007. doi: 10.1051/0004-6361:20077580.
- [109] D. Gruen, S. Seitz, F. Brimiouille, R. Kosyra, J. Koppenhoefer, C.-H. Lee, R. Bender, A. Riffeser, T. Eichner, T. Weidinger, and M. Bierchen. Weak lensing analysis of SZ-selected clusters of galaxies from the SPT and Planck surveys. *MNRAS*, 442:1507–1544, August 2014. doi: 10.1093/mnras/stu949.
- [110] H. Hoekstra, R. Herbonnet, A. Muzzin, A. Babul, A. Mahdavi, M. Viola, and M. Cacciato. The Canadian Cluster Comparison Project: detailed study of systematics and updated weak lensing masses. *MNRAS*, 449:685–714, May 2015. doi: 10.1093/mnras/stv275.
- [111] K. Umetsu, M. Sereno, E. Medezinski, M. Nonino, T. Mroczkowski, J. M. Diego, S. Ettori, N. Okabe, T. Broadhurst, and D. Lemze. Three-dimensional Multi-probe Analysis of the Galaxy Cluster A1689. *ApJ*, 806:207, June 2015. doi: 10.1088/0004-637X/806/2/207.
- [112] H. Dahle, N. Kaiser, R. J. Irgens, P. B. Lilje, and S. J. Maddox. Weak Gravitational Lensing by a Sample of X-Ray Luminous Clusters of Galaxies. I. The Data Set. *ApJS*, 139:313–368, April 2002.
- [113] E. S. Cypriano, L. J. Sodré, J. Kneib, and L. E. Campusano. Weak-Lensing Mass Distributions for 24 X-Ray Abell Clusters. *ApJ*, 613:95–108, September 2004.
- [114] A. Mahdavi, H. Hoekstra, A. Babul, C. Bildfell, T. Jeltema, and J. P. Henry. Joint Analysis of Cluster Observations. II. Chandra/XMM-Newton X-Ray and Weak Lensing Scaling Relations for a Sample of 50 Rich Clusters of Galaxies. *ApJ*, 767:116, April 2013. doi: 10.1088/0004-637X/767/2/116.
- [115] G. P. Smith, P. Mazzotta, N. Okabe, F. Ziparo, S. L. Mulroy, A. Babul, A. Finoguenov, I. G. McCarthy, M. Lieu, Y. M. Bahé, H. Bourdin, A. E. Evrard, T. Futamase, C. P. Haines, M. Jauzac, D. P. Marrone, R. Martino, P. E. May, J. E. Taylor, and K. Umetsu. LoCuSS: Testing hydrostatic equilibrium in galaxy clusters. *MNRAS*, 456:L74–L78, February 2016. doi: 10.1093/mnras/slv175.
- [116] G. A. Luppino and N. Kaiser. Detection of Weak Lensing by a Cluster of Galaxies at  $Z = 0.83$ . *ApJ*, 475:20–+, January 1997.
- [117] M. Lombardi, P. Rosati, J. P. Blakeslee, S. Ettori, R. Demarco, H. C. Ford, G. D. Illingworth, M. Clampin, G. F. Hartig, N. Benítez, T. J. Broadhurst, M. Franx, M. J. Jee, M. Postman, and R. L. White. Hubble Space Telescope ACS Weak-Lensing Analysis of the Galaxy Cluster RDCS 1252.9-2927 at  $z = 1.24$ . *ApJ*, 623:42–56, April 2005. doi: 10.1086/428427.
- [118] M. J. Jee, P. Rosati, H. C. Ford, K. S. Dawson, C. Lidman, S. Perlmutter, R. Demarco, V. Strazzullo, C. Mullis, H. Böhringer, and R. Fassbender. Hubble Space Telescope Weak-lensing Study of the Galaxy Cluster XMMU J2235.3 - 2557 at  $z \sim 1.4$ : A Surprisingly Massive Galaxy Cluster When the Universe is One-third of its Current Age. *ApJ*, 704:672–686, October 2009. doi: 10.1088/0004-637X/704/1/672.

- [119] M. J. Jee, J. P. Hughes, F. Menanteau, C. Sifón, R. Mandelbaum, L. F. Barrientos, L. Infante, and K. Y. Ng. Weighing "El Gordo" with a Precision Scale: Hubble Space Telescope Weak-lensing Analysis of the Merging Galaxy Cluster ACT-CL J0102-4915 at  $z = 0.87$ . *ApJ*, 785:20, April 2014. doi: 10.1088/0004-637X/785/1/20.
- [120] D. Coe, K. Umetsu, A. Zitrin, M. Donahue, E. Medezinski, M. Postman, M. Carrasco, T. Anguita, M. J. Geller, K. J. Rines, A. Diaferio, M. J. Kurtz, L. Bradley, A. Koekemoer, W. Zheng, M. Nonino, A. Molino, A. Mahdavi, D. Lemze, L. Infante, S. Ogaz, P. Melchior, O. Host, H. Ford, C. Grillo, P. Rosati, Y. Jiménez-Teja, J. Moustakas, T. Broadhurst, B. Ascaso, O. Lahav, M. Bartelmann, N. Benítez, R. Bouwens, O. Graur, G. Graves, S. Jha, S. Jouvel, D. Kelson, L. Moustakas, D. Maoz, M. Meneghetti, J. Merten, A. Riess, S. Rodney, and S. Seitz. CLASH: Precise New Constraints on the Mass Profile of the Galaxy Cluster A2261. *ApJ*, 757:22, September 2012. doi: 10.1088/0004-637X/757/1/22.
- [121] J. F. Navarro, C. S. Frenk, and S. D. M. White. The Structure of Cold Dark Matter Halos. *ApJ*, 462:563–+, May 1996.
- [122] J. F. Navarro, C. S. Frenk, and S. D. M. White. A Universal Density Profile from Hierarchical Clustering. *ApJ*, 490:493–+, December 1997.
- [123] D. Clowe and P. Schneider. Wide field weak lensing observations of A1689. *A&A*, 379:384–392, November 2001.
- [124] E. S. Sheldon, J. Annis, H. Böhringer, P. Fischer, J. A. Frieman, M. Joffe, D. Johnston, T. A. McKay, C. Miller, R. C. Nichol, A. Stebbins, W. Voges, S. F. Anderson, N. A. Bahcall, J. Brinkmann, R. Brunner, I. Csabai, M. Fukugita, G. S. Hennessy, Ž. Ivezić, R. H. Lupton, J. A. Munn, J. R. Pier, and D. G. York. Weak-Lensing Measurements of 42 SDSS/RASS Galaxy Clusters. *ApJ*, 554:881–887, June 2001.
- [125] K. Umetsu, E. Medezinski, M. Nonino, J. Merten, M. Postman, M. Meneghetti, M. Donahue, N. Czakon, A. Molino, S. Seitz, D. Gruen, D. Lemze, I. Balestra, N. Benítez, A. Biviano, T. Broadhurst, H. Ford, C. Grillo, A. Koekemoer, P. Melchior, A. Mercurio, J. Moustakas, P. Rosati, and A. Zitrin. CLASH: Weak-lensing Shear-and-magnification Analysis of 20 Galaxy Clusters. *ApJ*, 795:163, November 2014. doi: 10.1088/0004-637X/795/2/163.
- [126] H. Dahle, K. Pedersen, P. B. Lilje, S. J. Maddox, and N. Kaiser. Weak Gravitational Lensing by a Sample of X-Ray-luminous Clusters of Galaxies. III. Serendipitous Weak Lensing Detections of Dark and Luminous Mass Concentrations. *ApJ*, 591:662–676, July 2003.
- [127] N. Okabe, T. Futamase, M. Kajisawa, and R. Kuroshima. Subaru Weak-lensing Survey of Dark Matter Subhalos in the Coma Cluster: Subhalo Mass Function and Statistical Properties. *ApJ*, 784:90, April 2014. doi: 10.1088/0004-637X/784/2/90.
- [128] C. A. Metzler, M. White, M. Norman, and C. Loken. Weak Gravitational Lensing and Cluster Mass Estimates. *ApJL*, 520:L9–L12, July 1999.
- [129] L. J. King, P. Schneider, and V. Springel. Cluster mass profiles from weak lensing: The influence of substructure. *A&A*, 378:748–755, November 2001.
- [130] H. Hoekstra. How well can we determine cluster mass profiles from weak lensing? *MNRAS*, 339:1155–1162, March 2003.
- [131] P. Fischer. A New Weak-Lensing Analysis of MS 1224.7+2007. *AJ*, 117:2024–2033, May 1999.
- [132] T. Erben, L. van Waerbeke, Y. Mellier, P. Schneider, J.-C. Cuillandre, F. J. Castander, and M. Dantel-Fort. Mass-detection of a matter concentration projected near the cluster Abell 1942: Dark clump or high-redshift cluster? *A&A*, 355:23–36, March 2000.
- [133] K. Umetsu and T. Futamase. Detection of Dark Matter Concentrations in the Field of Cl 1604+4304 from Weak Lensing Analysis. *ApJL*, 539:L5–L8, August 2000.
- [134] M. E. Gray, R. S. Ellis, J. R. Lewis, R. G. McMahon, and A. E. Firth. Infrared constraints on the dark mass concentration observed in the cluster Abell 1942. *MNRAS*, 325:111–118, July 2001.
- [135] J.-M. Miralles, T. Erben, H. Hämmerle, P. Schneider, R. A. E. Fosbury, W. Freudling, N. Pirzkal, B. Jain, and S. D. M. White. A conspicuous tangential alignment of galaxies in a STIS Parallel Shear Survey field: A new dark-lens candidate? *A&A*, 388:68–73, June 2002.
- [136] T. Erben, J. M. Miralles, D. Clowe, M. Schirmer, P. Schneider, W. Freudling, N. Pirzkal, R. A. E. Fosbury, and B. Jain. A weak lensing analysis of a STIS dark-lens candidate. *A&A*, 410:45–52, October 2003.
- [137] P. Schneider. Detection of (dark) matter concentrations via weak gravitational lensing. *MNRAS*, 283:837–853, December 1996.
- [138] K. Reblinsky and M. Bartelmann. Projection effects in mass-selected galaxy-cluster samples. *A&A*, 345:1–16, May 1999.
- [139] M. White, L. van Waerbeke, and J. Mackey. Completeness in Weak-Lensing Searches for Clusters. *ApJ*, 575:640–649, August 2002.
- [140] M. Maturi, M. Meneghetti, M. Bartelmann, K. Dolag, and L. Moscardini. An optimal filter for the detection of galaxy clusters through weak lensing. *A&A*, 442:851–860, November 2005. doi: 10.1051/0004-6361:20042600.
- [141] F. Pace, M. Maturi, M. Meneghetti, M. Bartelmann, L. Moscardini, and K. Dolag. Testing the reliability of weak lensing cluster detections. *A&A*, 471:731–742, September 2007. doi: 10.1051/0004-6361:20077217.
- [142] G. Kruse and P. Schneider. Statistics of dark matter haloes expected from weak lensing surveys. *MNRAS*, 302:821–829, February 1999.
- [143] D. Wittman, J. A. Tyson, V. E. Margoniner, J. G. Cohen, and I. P. Dell'Antonio. Discovery of a Galaxy Cluster via Weak Lensing. *ApJL*, 557:L89–L92, August 2001.
- [144] M. Bartelmann, L. J. King, and P. Schneider. Weak-lensing halo numbers and dark-matter profiles. *A&A*, 378:361–369, November 2001.
- [145] S. Miyazaki, T. Hamana, K. Shimasaku, H. Furusawa, M. Doi, M. Hamabe, K. Imi, M. Kimura, Y. Komiyama, F. Nakata, N. Okada, S. Okamura, M. Ouchi, M. Sekiguchi, M. Yagi, and N. Yasuda. Searching for Dark Matter Halos in the Suprime-Cam 2 Square Degree Field. *ApJL*, 580:L97–L100, December 2002.
- [146] M. Schirmer, T. Erben, P. Schneider, C. Wolf, and K. Meisenheimer. GaBoDS: The Garching-Bonn Deep Survey. II. Confirmation of EIS cluster candidates by weak gravitational lensing. *A&A*, 420:75–78, June 2004.
- [147] M. Hetherscheidt, T. Erben, P. Schneider, R. Maoli, L. van Waerbeke, and Y. Mellier. Searching for galaxy clusters using the aperture mass statistics in 50 VLT fields. *A&A*, 442:43–61, October 2005. doi: 10.1051/0004-6361:20053339.
- [148] D. Wittman, I. P. Dell'Antonio, J. P. Hughes, V. E. Margoniner, J. A. Tyson, J. G. Cohen, and D. Norman. First Results on Shear-selected Clusters from the Deep Lens Survey: Optical Imaging, Spectroscopy, and X-Ray Follow-up. *ApJ*, 643:128–143, May 2006. doi: 10.1086/502621.
- [149] J. P. Dietrich, T. Erben, G. Lamer, P. Schneider, A. Schwöpe, J. Hartlap, and M. Maturi. BLOX: the Bonn lensing, optical, and X-ray selected galaxy clusters. I. Cluster catalog construction. *A&A*, 470:821–834, August 2007. doi: 10.1051/0004-6361:20077281.
- [150] R. Gavazzi and G. Soucail. Weak lensing survey of galaxy clusters in the CFHTLS Deep. *A&A*, 462:459–471, February 2007. doi: 10.1051/0004-6361:20065677.
- [151] S. Miyazaki, T. Hamana, R. S. Ellis, N. Kashikawa, R. J. Massey, J. Taylor, and A. Refregier. A Subaru Weak-Lensing Survey. I. Cluster Candidates and Spectroscopic Verification. *ApJ*, 669:714–728, November 2007. doi: 10.1086/521621.
- [152] M. Maturi, M. Schirmer, M. Meneghetti, M. Bartelmann, and L. Moscardini. Searching dark-matter halos in the GaBoDS survey. *A&A*, 462:473–479, February 2007. doi: 10.1051/0004-6361:20065323.
- [153] M. Schirmer, T. Erben, M. Hetherscheidt, and P. Schneider. GaBoDS: the Garching-Bonn Deep Survey. IX. A sample of 158 shear-selected mass concentration candidates. *A&A*, 462:875–887, February 2007. doi: 10.1051/0004-6361:20065955.
- [154] J. P. Dietrich and J. Hartlap. Cosmology with the shear-peak statistics. *MNRAS*, 402:1049–1058, February 2010. doi: 10.1111/j.1365-2966.2009.15948.x.

- [155] J. M. Kratochvil, Z. Haiman, and M. May. Probing cosmology with weak lensing peak counts. *Phys. Rev. D*, 81(4):043519, February 2010. doi: 10.1103/PhysRevD.81.043519.
- [156] M. Maturi, C. Angrick, F. Pace, and M. Bartelmann. An analytic approach to number counts of weak-lensing peak detections. *A&A*, 519:A23+, September 2010. doi: 10.1051/0004-6361/200912866.
- [157] M. Maturi, C. Fedeli, and L. Moscardini. Imprints of primordial non-Gaussianity on the number counts of cosmic shear peaks. *MNRAS*, 416:2527–2538, October 2011. doi: 10.1111/j.1365-2966.2011.18958.x.
- [158] H. Y. Shan, J.-P. Kneib, J. Comparat, E. Jullo, A. Charbonnier, T. Erben, M. Makler, B. Moraes, L. Van Waerbeke, F. Courbin, G. Meylan, C. Tao, and J. E. Taylor. Weak lensing mass map and peak statistics in Canada-France-Hawaii Telescope Stripe 82 survey. *MNRAS*, 442:2534–2542, August 2014. doi: 10.1093/mnras/stu1040.
- [159] C.-A. Lin and M. Kilbinger. A new model to predict weak-lensing peak counts. I. Comparison with N-body simulations. *A&A*, 576:A24, April 2015. doi: 10.1051/0004-6361/201425188.
- [160] M. Bartelmann, F. Perrotta, and C. Baccigalupi. Halo concentrations and weak-lensing number counts in dark energy cosmologies. *A&A*, 396:21–30, December 2002.
- [161] N. N. Weinberg and M. Kamionkowski. Weak gravitational lensing by dark clusters. *MNRAS*, 337:1269–1281, December 2002.
- [162] N. N. Weinberg and M. Kamionkowski. Constraining dark energy from the abundance of weak gravitational lenses. *MNRAS*, 341:251–262, May 2003.
- [163] L. Marian, R. E. Smith, S. Hilbert, and P. Schneider. The cosmological information of shear peaks: beyond the abundance. *MNRAS*, April 2013. doi: 10.1093/mnras/st552.
- [164] M. Kilbinger. Cosmology with cosmic shear observations: a review. *Reports on Progress in Physics*, 78(8):086901, July 2015. doi: 10.1088/0034-4885/78/8/086901.
- [165] R. Reischke, M. Maturi, and M. Bartelmann. Extreme value statistics of weak lensing shear peak counts. *MNRAS*, 456:641–653, February 2016. doi: 10.1093/mnras/stv2677.
- [166] J. R. Bond, L. Kofman, and D. Pogosyan. How filaments of galaxies are woven into the cosmic web. *Nature*, 380:603–606, April 1996. doi: 10.1038/380603a0.
- [167] H. Ebeling, E. Barrett, and D. Donovan. Discovery of a Large-Scale Filament Connected to the Massive Galaxy Cluster MACS J0717.5+3745 at  $z=0.551$ . *ApJ*, 609:L49–L52, July 2004. doi: 10.1086/422750.
- [168] J. M. Colberg, K. S. Krughoff, and A. J. Connolly. Intercluster filaments in a  $\Lambda$ CDM Universe. *MNRAS*, 359:272–282, May 2005. doi: 10.1111/j.1365-2966.2005.08897.x.
- [169] O. Hahn, C. M. Carollo, C. Porciani, and A. Dekel. The evolution of dark matter halo properties in clusters, filaments, sheets and voids. *MNRAS*, 381:41–51, October 2007. doi: 10.1111/j.1365-2966.2007.12249.x.
- [170] J. P. Dietrich, P. Schneider, D. Clowe, E. Romano-Díaz, and J. Kerp. Weak lensing study of dark matter filaments and application to the binary cluster  $z$ ASTROBJ $_i$ A 222/ $z$ ASTROBJ $_i$  and  $z$ ASTROBJ $_i$ A 223/ $z$ ASTROBJ $_i$ . *A&A*, 440:453–471, September 2005. doi: 10.1051/0004-6361:20041523.
- [171] J. M. G. Mead, L. J. King, and I. G. McCarthy. Probing the cosmic web: intercluster filament detection using gravitational lensing. *MNRAS*, 401:2257–2267, February 2010. doi: 10.1111/j.1365-2966.2009.15840.x.
- [172] M. Jauzac, E. Jullo, J.-P. Kneib, H. Ebeling, A. Leauthaud, C.-J. Ma, M. Limousin, R. Massey, and J. Richard. A weak lensing mass reconstruction of the large-scale filament feeding the massive galaxy cluster MACS J0717.5+3745. *MNRAS*, 426:3369–3384, November 2012. doi: 10.1111/j.1365-2966.2012.21966.x.
- [173] M. Maturi and J. Merten. Weak-lensing detection of intracluster filaments with ground-based data. *A&A*, 559:A112, November 2013. doi: 10.1051/0004-6361/201322007.
- [174] H. Hoekstra, H. K. C. Yee, and M. D. Gladders. Current status of weak gravitational lensing. *New Astronomy Review*, 46:767–781, November 2002.
- [175] Y. Mellier and L. van Waerbeke. Cosmological weak lensing. *Classical and Quantum Gravity*, 19:3505–3515, July 2002.
- [176] H. Hoekstra and B. Jain. Weak Gravitational Lensing and Its Cosmological Applications. *Annual Review of Nuclear and Particle Science*, 58:99–123, November 2008. doi: 10.1146/annurev.nucl.58.110707.171151.
- [177] D. Munshi, P. Valageas, L. van Waerbeke, and A. Heavens. Cosmology with weak lensing surveys. *PhysRep*, 462:67–121, June 2008. doi: 10.1016/j.physrep.2008.02.003.
- [178] R. D. Blandford, A. B. Saust, T. G. Brainerd, and J. V. Villumsen. The distortion of distant galaxy images by large-scale structure. *MNRAS*, 251:600–627, August 1991.
- [179] J. Miralda-Escudé. The correlation function of galaxy ellipticities produced by gravitational lensing. *ApJ*, 380:1–8, October 1991.
- [180] N. Kaiser. Weak gravitational lensing of distant galaxies. *ApJ*, 388:272–286, April 1992.
- [181] J. Mould, R. Blandford, J. Villumsen, T. Brainerd, I. Smail, T. Small, and W. Kells. A search for weak distortion of distant galaxy images by large-scale structure. *MNRAS*, 271:31–38, November 1994.
- [182] M. Bartelmann and P. Schneider. A large-scale structure model for gravitational lensing. *A&A*, 259:413–422, June 1992.
- [183] B. Jain and U. Seljak. Cosmological Model Predictions for Weak Lensing: Linear and Nonlinear Regimes. *ApJ*, 484:560–+, July 1997.
- [184] B. Jain, U. Seljak, and S. White. Ray-tracing Simulations of Weak Lensing by Large-Scale Structure. *ApJ*, 530:547–577, February 2000.
- [185] T. Hamana and Y. Mellier. Numerical study of the statistical properties of the lensing excursion angles. *MNRAS*, 327:169–176, October 2001.
- [186] C. Vale and M. White. Simulating Weak Lensing by Large-Scale Structure. *ApJ*, 592:699–709, August 2003.
- [187] S. Hilbert, J. Hartlap, S. D. M. White, and P. Schneider. Ray-tracing through the Millennium Simulation: Born corrections and lens-lens coupling in cosmic shear and galaxy-galaxy lensing. *A&A*, 499:31–43, May 2009. doi: 10.1051/0004-6361/200811054.
- [188] F. Bernardeau, L. van Waerbeke, and Y. Mellier. Weak lensing statistics as a probe of  $\{\Omega_{\text{MEGA}}\}$  and power spectrum. *A&A*, 322:1–18, June 1997.
- [189] N. Kaiser. Weak Lensing and Cosmology. *ApJ*, 498:26–+, May 1998.
- [190] L. van Waerbeke, F. Bernardeau, and Y. Mellier. Efficiency of weak lensing surveys to probe cosmological models. *A&A*, 342:15–33, February 1999.
- [191] P. Schneider, L. van Waerbeke, Y. Mellier, B. Jain, S. Seitz, and B. Fort. Detection of shear due to weak lensing by large-scale structure. *A&A*, 333:767–778, May 1998.
- [192] D. J. Bacon, A. R. Refregier, and R. S. Ellis. Detection of weak gravitational lensing by large-scale structure. *MNRAS*, 318:625–640, October 2000.
- [193] L. Van Waerbeke, Y. Mellier, T. Erben, J. C. Cuillandre, F. Bernardeau, R. Maoli, E. Bertin, H. J. Mc Cracken, O. Le Fèvre, B. Fort, M. Dantel-Fort, B. Jain, and P. Schneider. Detection of correlated galaxy ellipticities from CFHT data: first evidence for gravitational lensing by large-scale structures. *A&A*, 358:30–44, June 2000.
- [194] D. M. Wittman, J. A. Tyson, D. Kirkman, I. Dell’Antonio, and G. Bernstein. Detection of weak gravitational lensing distortions of distant galaxies by cosmic dark matter at large scales. *Nat*, 405:143–148, May 2000.
- [195] R. Maoli, L. Van Waerbeke, Y. Mellier, P. Schneider, B. Jain, F. Bernardeau, T. Erben, and B. Fort. Cosmic shear analysis in 50 uncorrelated VLT fields. Implications for  $\Omega_0$ ,  $\sigma_8$ . *A&A*, 368:766–775, March 2001.

- [196] L. Van Waerbeke, T. Hamana, R. Scoccimarro, S. Colombi, and F. Bernardeau. Weak lensing predictions at intermediate scales. *MNRAS*, 322:918–926, April 2001.
- [197] L. Van Waerbeke, Y. Mellier, M. Radovich, E. Bertin, M. Dantel-Fort, H. J. McCracken, O. Le Fèvre, S. Foucaud, J.-C. Cuillandre, T. Erben, B. Jain, P. Schneider, F. Bernardeau, and B. Fort. Cosmic shear statistics and cosmology. *A&A*, 374:757–769, August 2001.
- [198] F. Bernardeau, Y. Mellier, and L. van Waerbeke. Detection of non-Gaussian signatures in the VIRMOS-DESCART lensing survey. *A&A*, 389:L28–L32, July 2002.
- [199] M. Kilbinger and P. Schneider. Cosmological parameters from combined second- and third-order aperture mass statistics of cosmic shear. *A&A*, 442:69–83, October 2005. doi: 10.1051/0004-6361:20053531.
- [200] T. Erben, L. Van Waerbeke, E. Bertin, Y. Mellier, and P. Schneider. How accurately can we measure weak gravitational shear? *A&A*, 366:717–735, February 2001.
- [201] W. Hu and M. White. Power Spectra Estimation for Weak Lensing. *ApJ*, 554:67–73, June 2001.
- [202] A. Cooray and W. Hu. Power Spectrum Covariance of Weak Gravitational Lensing. *ApJ*, 554:56–66, June 2001.
- [203] P. Schneider, L. van Waerbeke, M. Kilbinger, and Y. Mellier. Analysis of two-point statistics of cosmic shear. I. Estimators and covariances. *A&A*, 396:1–19, December 2002.
- [204] E. Semboloni, L. van Waerbeke, C. Heymans, T. Hamana, S. Colombi, M. White, and Y. Mellier. Cosmic variance of weak lensing surveys in the non-Gaussian regime. *MNRAS*, 375:L6–L10, February 2007. doi: 10.1111/j.1745-3933.2006.00266.x.
- [205] B. Joachimi, P. Schneider, and T. Eifler. Analysis of two-point statistics of cosmic shear. III. Covariances of shear measures made easy. *A&A*, 477:43–54, January 2008. doi: 10.1051/0004-6361:20078400.
- [206] J. Hartlap, T. Schrabback, P. Simon, and P. Schneider. The non-Gaussianity of the cosmic shear likelihood or how odd is the Chandra Deep Field South? *A&A*, 504:689–703, September 2009. doi: 10.1051/0004-6361/200911697.
- [207] H. Hoekstra, H. K. C. Yee, M. D. Gladders, L. F. Barrientos, P. B. Hall, and L. Infante. A Measurement of Weak Lensing by Large-Scale Structure in Red-Sequence Cluster Survey Fields. *ApJ*, 572:55–65, June 2002.
- [208] D. J. Bacon, R. J. Massey, A. R. Refregier, and R. S. Ellis. Joint cosmic shear measurements with the Keck and William Herschel Telescopes. *MNRAS*, 344:673–685, September 2003.
- [209] M. L. Brown, A. N. Taylor, D. J. Bacon, M. E. Gray, S. Dye, K. Meisenheimer, and C. Wolf. The shear power spectrum from the COMBO-17 survey. *MNRAS*, 341:100–118, May 2003.
- [210] T. Hamana, S. Miyazaki, K. Shimasaku, H. Furusawa, M. Doi, M. Hamabe, K. Imi, M. Kimura, Y. Komiyama, F. Nakata, N. Okada, S. Okamura, M. Ouchi, M. Sekiguchi, M. Yagi, and N. Yasuda. Cosmic Shear Statistics in the Suprime-Cam 2.1 Square Degree Field: Constraints on  $\Omega_m$  and  $\sigma_8$ . *ApJ*, 597:98–110, November 2003.
- [211] M. Jarvis, G. M. Bernstein, P. Fischer, D. Smith, B. Jain, J. A. Tyson, and D. Wittman. Weak-Lensing Results from the 75 Square Degree Cerro Tololo Inter-American Observatory Survey. *AJ*, 125:1014–1032, March 2003.
- [212] J. Rhodes, A. Refregier, N. R. Collins, J. P. Gardner, E. J. Groth, and R. S. Hill. Measurement of Cosmic Shear with the Space Telescope Imaging Spectrograph. *ApJ*, 605:29–36, April 2004.
- [213] C. Heymans, M. L. Brown, M. Barden, J. A. R. Caldwell, K. Jahnke, C. Y. Peng, H.-W. Rix, A. Taylor, S. V. W. Beckwith, E. F. Bell, A. Borch, B. Häußler, S. Jogee, D. H. McIntosh, K. Meisenheimer, S. F. Sánchez, R. Somerville, L. Wisotzki, and C. Wolf. Cosmological weak lensing with the HST GEMS survey. *MNRAS*, 361:160–176, July 2005. doi: 10.1111/j.1365-2966.2005.09152.x.
- [214] R. Massey, A. Refregier, D. J. Bacon, R. Ellis, and M. L. Brown. An enlarged cosmic shear survey with the William Herschel Telescope. *MNRAS*, 359:1277–1286, June 2005. doi: 10.1111/j.1365-2966.2005.09011.x.
- [215] L. Van Waerbeke, Y. Mellier, and H. Hoekstra. Dealing with systematics in cosmic shear studies: New results from the VIRMOS-DESCART survey. *A&A*, 429:75–84, January 2005.
- [216] H. Hoekstra, Y. Mellier, L. van Waerbeke, E. Semboloni, L. Fu, M. J. Hudson, L. C. Parker, I. Tereno, and K. Benabed. First Cosmic Shear Results from the Canada-France-Hawaii Telescope Wide Synoptic Legacy Survey. *ApJ*, 647:116–127, August 2006. doi: 10.1086/503249.
- [217] E. Semboloni, Y. Mellier, L. van Waerbeke, H. Hoekstra, I. Tereno, K. Benabed, S. D. J. Gwyn, L. Fu, M. J. Hudson, R. Maoli, and L. C. Parker. Cosmic shear analysis with CFHTLS deep data. *A&A*, 452:51–61, June 2006. doi: 10.1051/0004-6361:20054479.
- [218] J. Benjamin, C. Heymans, E. Semboloni, L. van Waerbeke, H. Hoekstra, T. Erben, M. D. Gladders, M. Hetterscheidt, Y. Mellier, and H. K. C. Yee. Cosmological constraints from the 100-deg<sup>2</sup> weak-lensing survey. *MNRAS*, 381:702–712, October 2007. doi: 10.1111/j.1365-2966.2007.12202.x.
- [219] M. Hetterscheidt, P. Simon, M. Schirmer, H. Hildebrandt, T. Schrabback, T. Erben, and P. Schneider. GaBoDS: The Garching-Bonn deep survey. VII. Cosmic shear analysis. *A&A*, 468:859–876, June 2007. doi: 10.1051/0004-6361:20065885.
- [220] T. D. Kitching, A. F. Heavens, A. N. Taylor, M. L. Brown, K. Meisenheimer, C. Wolf, M. E. Gray, and D. J. Bacon. Cosmological constraints from COMBO-17 using 3D weak lensing. *MNRAS*, 376:771–778, April 2007. doi: 10.1111/j.1365-2966.2007.11473.x.
- [221] R. Massey, J. Rhodes, A. Leauthaud, P. Capak, R. Ellis, A. Koekemoer, A. Réfrégier, N. Scoville, J. E. Taylor, J. Albert, J. Bergé, C. Heymans, D. Johnston, J.-P. Kneib, Y. Mellier, B. Mobasher, E. Semboloni, P. Shopbell, L. Tasca, and L. Van Waerbeke. COSMOS: Three-dimensional Weak Lensing and the Growth of Structure. *ApJS*, 172:239–253, September 2007. doi: 10.1086/516599.
- [222] T. Schrabback, T. Erben, P. Simon, J.-M. Miralles, P. Schneider, C. Heymans, T. Eifler, R. A. E. Fosbury, W. Freudling, M. Hetterscheidt, H. Hildebrandt, and N. Pirzkal. Cosmic shear analysis of archival HST/ACS data. I. Comparison of early ACS pure parallel data to the HST/GEMS survey. *A&A*, 468:823–847, June 2007. doi: 10.1051/0004-6361:20065898.
- [223] L. Fu, E. Semboloni, H. Hoekstra, M. Kilbinger, L. van Waerbeke, I. Tereno, Y. Mellier, C. Heymans, J. Coupon, K. Benabed, J. Benjamin, E. Bertin, O. Doré, M. J. Hudson, O. Ilbert, R. Maoli, C. Marmo, H. J. McCracken, and B. Ménard. Very weak lensing in the CFHTLS wide: cosmology from cosmic shear in the linear regime. *A&A*, 479:9–25, February 2008. doi: 10.1051/0004-6361:20078522.
- [224] C. Heymans, L. Van Waerbeke, L. Miller, T. Erben, H. Hildebrandt, H. Hoekstra, T. D. Kitching, Y. Mellier, P. Simon, C. Bonnett, J. Coupon, L. Fu, J. Harnois Dérapas, M. J. Hudson, M. Kilbinger, K. Kuijken, B. Rowe, T. Schrabback, E. Semboloni, E. van Uitert, S. Vafaei, and M. Velander. CFHTLenS: the Canada-France-Hawaii Telescope Lensing Survey. *MNRAS*, 427:146–166, November 2012. doi: 10.1111/j.1365-2966.2012.21952.x.
- [225] L. Van Waerbeke, J. Benjamin, T. Erben, C. Heymans, H. Hildebrandt, H. Hoekstra, T. D. Kitching, Y. Mellier, L. Miller, J. Coupon, J. Harnois-Dérapas, L. Fu, M. Hudson, M. Kilbinger, K. Kuijken, B. Rowe, T. Schrabback, E. Semboloni, S. Vafaei, E. van Uitert, and M. Velander. CFHTLenS: mapping the large-scale structure with gravitational lensing. *MNRAS*, 433:3373–3388, August 2013. doi: 10.1093/mnras/stt971.
- [226] J. T. A. de Jong, G. A. Verdoes Kleijn, K. H. Kuijken, and E. A. Valentijn. The Kilo-Degree Survey. *Experimental Astronomy*, 35:25–44, January 2013. doi: 10.1007/s10686-012-9306-1.
- [227] Dark Energy Survey Collaboration, T. Abbott, F. B. Abdalla, J. Aleksić, S. Allam, A. Amara, D. Bacon, E. Balbinot, M. Banerji, K. Bechtol, A. Benoit-Lévy, G. M. Bernstein, E. Bertin, J. Blazek, C. Bonnett, S. Bridle, D. Brooks, R. J. Brunner, E. Buckley-Geer, D. L. Burke, G. B. Caminha, D. Capozzi, J. Carlsen, A. Carnero-Rosell, M. Carollo,

- M. Carrasco-Kind, J. Carretero, F. J. Castander, L. Clerkin, T. Collett, C. Conselice, M. Crocce, C. E. Cunha, C. B. D'Andrea, L. N. da Costa, T. M. Davis, S. Desai, H. T. Diehl, J. P. Dietrich, S. Dodelson, P. Doel, A. Drlica-Wagner, J. Estrada, J. Etherington, A. E. Evrard, J. Fabbri, D. A. Finley, B. Flaugher, R. J. Foley, P. Fosalba, J. Frieman, J. García-Bellido, E. Gaztanaga, D. W. Gerdes, T. Giannantonio, D. A. Goldstein, D. Gruen, R. A. Gruendl, P. Guarnieri, G. Gutierrez, W. Hartley, K. Honscheid, B. Jain, D. J. James, T. Jeltema, S. Jouvel, R. Kessler, A. King, D. Kirk, R. Kron, K. Kuehn, N. Kuropatkin, O. Lahav, T. S. Li, M. Lima, H. Lin, M. A. G. Maia, M. Makler, M. Manera, C. Maraston, J. L. Marshall, P. Martini, R. G. McMahon, P. Melchior, A. Merson, C. J. Miller, R. Miquel, J. J. Mohr, X. Morice-Atkinson, K. Naidoo, E. Neilsen, R. C. Nichol, B. Nord, R. Ogando, F. Ostrovski, A. Palmese, A. Papadopoulos, H. V. Peiris, J. Peoples, W. J. Percival, A. A. Plazas, S. L. Reed, A. Refregier, A. K. Romer, A. Roodman, A. Ross, E. Rozo, E. S. Rykoff, I. Sadeh, M. Sako, C. Sánchez, E. Sanchez, B. Santiago, V. Scarpine, M. Schubnell, I. Sevilla-Noarbe, E. Sheldon, M. Smith, R. C. Smith, M. Soares-Santos, F. Sobreira, M. Soumagnac, E. Suchyta, M. Sullivan, M. Swanson, G. Tarle, J. Thaler, D. Thomas, R. C. Thomas, D. Tucker, J. D. Vieira, V. Vikram, A. R. Walker, R. H. Wechsler, J. Weller, W. Wester, L. Whiteway, H. Wilcox, B. Yanny, Y. Zhang, and J. Zuntz. The Dark Energy Survey: more than dark energy - an overview. *MNRAS*, 460:1270–1299, August 2016. doi: 10.1093/mnras/stw641.
- [228] R. Laureijs, P. Gondoin, L. Duvet, G. Saavedra Criado, J. Hoar, J. Amiaux, J.-L. Auguères, R. Cole, M. Cropper, A. Ealet, P. Ferruit, I. Escudero Sanz, K. Jahnke, R. Kohley, T. Maciaszek, Y. Mellier, T. Oosterbroek, F. Pasian, M. Sauvage, R. Scaramella, M. Sirianni, and L. Valenziano. Euclid: ESA's mission to map the geometry of the dark universe. In *Space Telescopes and Instrumentation 2012: Optical, Infrared, and Millimeter Wave*, volume 8442 of *Proc. SPIE*, page 84420T, September 2012. doi: 10.1117/12.926496.
- [229] C. Chang, M. Jarvis, B. Jain, S. M. Kahn, D. Kirkby, A. Connolly, S. Krughoff, E.-H. Peng, and J. R. Peterson. The effective number density of galaxies for weak lensing measurements in the LSST project. *MNRAS*, 434:2121–2135, September 2013. doi: 10.1093/mnras/stt1156.
- [230] M. Brown, D. Bacon, S. Camera, I. Harrison, B. Joachimi, R. B. Metcalf, A. Poursidou, K. Takahashi, J. Zuntz, F. B. Abdalla, S. Bridle, M. Jarvis, T. Kitching, L. Miller, and P. Patel. Weak gravitational lensing with the Square Kilometre Array. *Advancing Astrophysics with the Square Kilometre Array (AASKA14)*, art. 23, 2015.
- [231] A. Bonaldi, I. Harrison, S. Camera, and M. L. Brown. SKA weak lensing- II. Simulated performance and survey design considerations. *MNRAS*, 463:3686–3698, December 2016. doi: 10.1093/mnras/stw2104.
- [232] P. Patel. Weak Lensing with Radio Continuum Surveys. *ArXiv e-prints*, February 2016.
- [233] H. Hildebrandt, M. Viola, C. Heymans, S. Joudaki, K. Kuijken, C. Blake, T. Erben, B. Joachimi, D. Klaes, L. Miller, C. B. Morrison, R. Nakajima, G. Verdoes Kleijn, A. Amon, A. Choi, G. Covone, J. T. A. de Jong, A. Dvornik, I. Fenech Conti, A. Grado, J. Harnois-Déraps, R. Herbonnet, H. Hoekstra, F. Köhlinger, J. McFarland, A. Mead, J. Merten, N. Napolitano, J. A. Peacock, M. Radovich, P. Schneider, P. Simon, E. A. Valentijn, J. L. van den Busch, E. van Uitert, and L. Van Waerbeke. KiDS-450: Cosmological parameter constraints from tomographic weak gravitational lensing. *ArXiv e-prints*, June 2016.
- [234] C. Heymans, E. Grocutt, A. Heavens, M. Kilbinger, T. D. Kitching, F. Simpson, J. Benjamin, T. Erben, H. Hildebrandt, H. Hoekstra, Y. Mellier, L. Miller, L. Van Waerbeke, M. L. Brown, J. Coupon, L. Fu, J. Harnois-Déraps, M. J. Hudson, K. Kuijken, B. Rowe, T. Schrabback, E. Semboloni, S. Vafaei, and M. Velander. CFHTLenS tomographic weak lensing cosmological parameter constraints: Mitigating the impact of intrinsic galaxy alignments. *MNRAS*, 432:2433–2453, July 2013. doi: 10.1093/mnras/stt601.
- [235] S. Dodelson, E. W. Kolb, S. Matarrese, A. Riotto, and P. Zhang. Second order geodesic corrections to cosmic shear. *PRD*, 72(10):103004–+, November 2005. doi: 10.1103/PhysRevD.72.103004.
- [236] C. Shapiro and A. Cooray. The Born and lens lens corrections to weak gravitational lensing angular power spectra. *Journal of Cosmology and Astro-Particle Physics*, 3:7–+, March 2006. doi: 10.1088/1475-7516/2006/03/007.
- [237] P. Schneider, L. van Waerbeke, and Y. Mellier. B-modes in cosmic shear from source redshift clustering. *A&A*, 389:729–741, July 2002.
- [238] H. Hoekstra. The effect of imperfect models of point spread function anisotropy on cosmic shear measurements. *MNRAS*, 347:1337–1344, February 2004.
- [239] M. Kilbinger, P. Schneider, and T. Eifler. E- and B-mode mixing from incomplete knowledge of the shear correlation. *A&A*, 457:15–19, October 2006. doi: 10.1051/0004-6361:20065495.
- [240] P. Schneider and M. Kilbinger. The ring statistics - how to separate E- and B-modes of cosmic shear correlation functions on a finite interval. *A&A*, 462:841–849, February 2007. doi: 10.1051/0004-6361:20065532.
- [241] L. Fu and M. Kilbinger. A new cosmic shear function: optimized E-/B-mode decomposition on a finite interval. *MNRAS*, 401:1264–1274, January 2010. doi: 10.1111/j.1365-2966.2009.15720.x.
- [242] J. Guzik and G. Bernstein. Inhomogeneous systematic signals in cosmic shear observations. *PRD*, 72(4):043503–+, August 2005. doi: 10.1103/PhysRevD.72.043503.
- [243] B. Jain, M. Jarvis, and G. Bernstein. PSF anisotropy and systematic errors in weak lensing surveys. *Journal of Cosmology and Astro-Particle Physics*, 2:1–+, February 2006. doi: 10.1088/1475-7516/2006/02/001.
- [244] Y. P. Jing, P. Zhang, W. P. Lin, L. Gao, and V. Springel. The Influence of Baryons on the Clustering of Matter and Weak-Lensing Surveys. *ApJL*, 640:L119–L122, April 2006. doi: 10.1086/503547.
- [245] L. van Waerbeke, M. White, H. Hoekstra, and C. Heymans. Redshift and shear calibration: Impact on cosmic shear studies and survey design. *Astroparticle Physics*, 26:91–101, September 2006. doi: 10.1016/j.astropartphys.2006.05.008.
- [246] K. Osato, M. Shirasaki, and N. Yoshida. Impact of Baryonic Processes on Weak-lensing Cosmology: Power Spectrum, Nonlocal Statistics, and Parameter Bias. *ApJ*, 806:186, June 2015. doi: 10.1088/0004-637X/806/2/186.
- [247] M. A. Troxel and M. Ishak. The intrinsic alignment of galaxies and its impact on weak gravitational lensing in an era of precision cosmology. *Phys. Rep.*, 558:1–59, February 2015. doi: 10.1016/j.physrep.2014.11.001.
- [248] R. A. C. Croft and C. A. Metzler. Weak-Lensing Surveys and the Intrinsic Correlation of Galaxy Ellipticities. *ApJ*, 545:561–571, December 2000.
- [249] A. Heavens, A. Refregier, and C. Heymans. Intrinsic correlation of galaxy shapes: implications for weak lensing measurements. *MNRAS*, 319:649–656, December 2000.
- [250] P. Catelan, M. Kamionkowski, and R. D. Blandford. Intrinsic and extrinsic galaxy alignment. *MNRAS*, 320:L7–L13, January 2001.
- [251] R. G. Crittenden, P. Natarajan, U. Pen, and T. Theuns. Spin-induced Galaxy Alignments and Their Implications for Weak-Lensing Measurements. *ApJ*, 559:552–571, October 2001.
- [252] M. L. Brown, A. N. Taylor, N. C. Hambly, and S. Dye. Measurement of intrinsic alignments in galaxy ellipticities. *MNRAS*, 333:501–509, July 2002.
- [253] Y. P. Jing. Intrinsic correlation of halo ellipticity and its implications for large-scale weak lensing surveys. *MNRAS*, 335:L89–L93, October 2002.
- [254] J. Lee and U. Pen. Detection of Galaxy Spin Alignments in the Point Source Catalog Redshift Survey Shear Field. *ApJL*, 567:L111–L114, March 2002.
- [255] J. Lee. The Intrinsic Inclination of Galaxies Embedded in Cosmic Sheets and Its Cosmological Implications: An Analytic Calculation. *ApJL*, 614:L1–L4, October 2004.
- [256] A. Faltenbacher, C. Li, S. D. M. White, Y.-P. Jing, Shu-DeMao, and J. Wang. Alignment between galaxies and large-scale structure. *Research in Astronomy and Astrophysics*, 9:41–58, January 2009. doi: 10.1088/1674-4527/9/1/004.

- [257] M. L. Brown and R. A. Battye. Polarization as an indicator of intrinsic alignment in radio weak lensing. *MNRAS*, 410:2057–2074, January 2011. doi: 10.1111/j.1365-2966.2010.17583.x.
- [258] B. Joachimi, R. Mandelbaum, F. B. Abdalla, and S. L. Bridle. Constraints on intrinsic alignment contamination of weak lensing surveys using the MegaZ-LRG sample. *A&A*, 527:A26, March 2011. doi: 10.1051/0004-6361/201015621.
- [259] R. Mandelbaum, C. Blake, S. Bridle, F. B. Abdalla, S. Brough, M. Colless, W. Couch, S. Croom, T. Davis, M. J. Drinkwater, K. Forster, K. Glazebrook, B. Jelliffe, R. J. Jurek, I.-H. Li, B. Madore, C. Martin, K. Pimbblet, G. B. Poole, M. Pracy, R. Sharp, E. Wisnioski, D. Woods, and T. Wyder. The WiggleZ Dark Energy Survey: direct constraints on blue galaxy intrinsic alignments at intermediate redshifts. *MNRAS*, 410:844–859, January 2011. doi: 10.1111/j.1365-2966.2010.17485.x.
- [260] D. Kirk, A. Rassat, O. Host, and S. Bridle. The cosmological impact of intrinsic alignment model choice for cosmic shear. *MNRAS*, 424:1647–1657, August 2012. doi: 10.1111/j.1365-2966.2012.21099.x.
- [261] F. Capranico, P. M. Merkel, and B. M. Schäfer. Intrinsic ellipticity correlations of galaxies: models, likelihoods and interplay with weak lensing. *MNRAS*, 435:194–206, October 2013. doi: 10.1093/mnras/stt1269.
- [262] B. Joachimi, E. Semboloni, S. Hilbert, P. E. Bett, J. Hartlap, H. Hoekstra, and P. Schneider. Intrinsic galaxy shapes and alignments - II. Modelling the intrinsic alignment contamination of weak lensing surveys. *MNRAS*, 436:819–838, November 2013. doi: 10.1093/mnras/stt1618.
- [263] P. M. Merkel and B. M. Schäfer. Intrinsic alignments and 3d weak gravitational lensing. *MNRAS*, 434:1808–1820, September 2013. doi: 10.1093/mnras/stt1151.
- [264] A. Giahi-Saravani and B. M. Schäfer. Weak gravitational lensing of intrinsically aligned galaxies. *MNRAS*, 437:1847–1857, January 2014. doi: 10.1093/mnras/stt2016.
- [265] P. M. Merkel and B. M. Schäfer. A theoretical estimate of intrinsic ellipticity bispectra induced by angular momenta alignments. *MNRAS*, 445:2918–2929, December 2014. doi: 10.1093/mnras/stu1945.
- [266] D. Kirk, M. L. Brown, H. Hoekstra, B. Joachimi, T. D. Kitching, R. Mandelbaum, C. Sifón, M. Cacciato, A. Choi, A. Kiessling, A. Leonard, A. Rassat, and B. M. Schäfer. Galaxy Alignments: Observations and Impact on Cosmology. *Space Sci. Rev.*, 193:139–211, November 2015. doi: 10.1007/s11214-015-0213-4.
- [267] T. Schrabback, S. Hilbert, H. Hoekstra, P. Simon, E. van Uitert, T. Erben, C. Heymans, H. Hildebrandt, T. D. Kitching, Y. Mellier, L. Miller, L. Van Waerbeke, P. Bett, J. Coupon, L. Fu, M. J. Hudson, B. Joachimi, M. Kilbinger, and K. Kuijken. CFHTLenS: weak lensing constraints on the ellipticity of galaxy-scale matter haloes and the galaxy-halo misalignment. *MNRAS*, 454:1432–1452, December 2015. doi: 10.1093/mnras/stv2053.
- [268] S. Singh, R. Mandelbaum, and S. More. Intrinsic alignments of SDSS-III BOSS LOWZ sample galaxies. *MNRAS*, 450:2195–2216, June 2015. doi: 10.1093/mnras/stv778.
- [269] C. Sifón, H. Hoekstra, M. Cacciato, M. Viola, F. Köhlinger, R. F. J. van der Burg, D. J. Sand, and M. L. Graham. Constraints on the alignment of galaxies in galaxy clusters from  $\sim 14\,000$  spectroscopic members. *A&A*, 575:A48, March 2015. doi: 10.1051/0004-6361/201424435.
- [270] L. King and P. Schneider. Suppressing the contribution of intrinsic galaxy alignments to the shear two-point correlation function. *A&A*, 396:411–418, December 2002.
- [271] C. Heymans and A. Heavens. Weak gravitational lensing: reducing the contamination by intrinsic alignments. *MNRAS*, 339:711–720, March 2003.
- [272] C. Heymans, M. Brown, A. Heavens, K. Meisenheimer, A. Taylor, and C. Wolf. Weak lensing with COMBO-17: estimation and removal of intrinsic alignments. *MNRAS*, 347:895–908, January 2004.
- [273] C. M. Hirata and U. Seljak. Intrinsic alignment-lensing interference as a contaminant of cosmic shear. *Phys. Rev. D*, 70(6):063526–+, September 2004.
- [274] R. Mandelbaum, C. M. Hirata, M. Ishak, U. Seljak, and J. Brinkmann. Detection of large-scale intrinsic ellipticity-density correlation from the Sloan Digital Sky Survey and implications for weak lensing surveys. *MNRAS*, 367:611–626, April 2006. doi: 10.1111/j.1365-2966.2005.09946.x.
- [275] C. M. Hirata, R. Mandelbaum, M. Ishak, U. Seljak, R. Nichol, K. A. Pimbblet, N. P. Ross, and D. Wake. Intrinsic galaxy alignments from the 2SLAQ and SDSS surveys: luminosity and redshift scalings and implications for weak lensing surveys. *MNRAS*, 381:1197–1218, November 2007. doi: 10.1111/j.1365-2966.2007.12312.x.
- [276] W. Hu and M. Tegmark. Weak Lensing: Prospects for Measuring Cosmological Parameters. *ApJL*, 514:L65–L68, April 1999.
- [277] C. R. Contaldi, H. Hoekstra, and A. Lewis. Joint Cosmic Microwave Background and Weak Lensing Analysis: Constraints on Cosmological Parameters. *Physical Review Letters*, 90(22):221303–+, June 2003.
- [278] I. Tereno, O. Doré, L. van Waerbeke, and Y. Mellier. Joint cosmological parameters forecast from CFHTLS-cosmic shear and CMB data. *A&A*, 429:383–398, January 2005.
- [279] T. Zhang, U. Pen, P. Zhang, and J. Dubinski. Optimal Weak-Lensing Skewness Measurements. *ApJ*, 598:818–826, December 2003.
- [280] M. Takada and B. Jain. Three-point correlations in weak lensing surveys: model predictions and applications. *MNRAS*, 344:857–886, September 2003.
- [281] D. Dolney, B. Jain, and M. Takada. Effects of halo substructure on the power spectrum and bispectrum. *MNRAS*, 352:1019–1027, August 2004.
- [282] A. Heavens. 3D weak lensing. *MNRAS*, 343:1327–1334, August 2003.
- [283] U. Pen. Beating lensing cosmic variance with galaxy tomography. *MNRAS*, 350:1445–1448, June 2004.
- [284] P. Simon, L. J. King, and P. Schneider. The covariance of cosmic shear correlation functions and cosmological parameter estimates using redshift information. *A&A*, 417:873–885, April 2004.
- [285] A. N. Taylor, D. J. Bacon, M. E. Gray, C. Wolf, K. Meisenheimer, S. Dye, A. Borch, M. Kleinheinrich, Z. Kovacs, and L. Wisotzki. Mapping the 3D dark matter with weak lensing in COMBO-17. *MNRAS*, 353:1176–1196, October 2004.
- [286] J. Benjamin, L. Van Waerbeke, C. Heymans, M. Kilbinger, T. Erben, H. Hildebrandt, H. Hoekstra, T. D. Kitching, Y. Mellier, L. Miller, B. Rowe, T. Schrabback, F. Simpson, J. Coupon, L. Fu, J. Harnois-Déraps, M. J. Hudson, K. Kuijken, E. Semboloni, S. Vafaei, and M. Velander. CFHTLenS tomographic weak lensing: quantifying accurate redshift distributions. *MNRAS*, 431:1547–1564, May 2013. doi: 10.1093/mnras/stt276.
- [287] T. D. Kitching, A. F. Heavens, J. Alsing, T. Erben, C. Heymans, H. Hildebrandt, H. Hoekstra, A. Jaffe, A. Kiessling, Y. Mellier, L. Miller, L. van Waerbeke, J. Benjamin, J. Coupon, L. Fu, M. J. Hudson, M. Kilbinger, K. Kuijken, B. T. P. Rowe, T. Schrabback, E. Semboloni, and M. Velander. 3D cosmic shear: cosmology from CFHTLenS. *MNRAS*, 442:1326–1349, August 2014. doi: 10.1093/mnras/stu934.
- [288] D. Huterer. Weak lensing and dark energy. *Phys. Rev. D*, 65(6):063001–+, March 2002.
- [289] D. Munshi and Y. Wang. How Sensitive Are Weak Lensing Statistics to Dark Energy Content? *ApJ*, 583:566–574, February 2003.
- [290] K. Benabed and L. van Waerbeke. Constraining dark energy evolution with gravitational lensing by large scale structures. *Phys. Rev. D*, 70(12):123515–+, December 2004.
- [291] T. Chang, A. Refregier, and D. J. Helfand. Weak Lensing by Large-Scale Structure with the FIRST Radio Survey. *ApJ*, 617:794–810, December 2004.
- [292] R. Massey, J. Rhodes, A. Refregier, J. Albert, D. Bacon, G. Bernstein, R. Ellis, B. Jain, T. McKay, S. Perlmutter, and A. Taylor. Weak Lensing from Space. II. Dark Matter Mapping. *AJ*, 127:3089–3101, June 2004.

- [293] U. Pen. Gravitational lensing of epoch-of-reionization gas. *New Astronomy*, 9:417–424, July 2004.
- [294] A. Refregier, R. Massey, J. Rhodes, R. Ellis, J. Albert, D. Bacon, G. Bernstein, T. McKay, and S. Perlmutter. Weak Lensing from Space. III. Cosmological Parameters. *AJ*, 127:3102–3114, June 2004.
- [295] L. J. King. Cosmic shear as a tool for precision cosmology: minimizing intrinsic galaxy alignment-lensing interference. *A&A*, 441:47–53, October 2005. doi: 10.1051/0004-6361:20053330.
- [296] A. F. Heavens, T. D. Kitching, and A. N. Taylor. Measuring dark energy properties with 3D cosmic shear. *MNRAS*, 373:105–120, November 2006. doi: 10.1111/j.1365-2966.2006.11006.x.
- [297] S. Bridle and L. King. Dark energy constraints from cosmic shear power spectra: impact of intrinsic alignments on photometric redshift requirements. *New Journal of Physics*, 9:444–+, December 2007. doi: 10.1088/1367-2630/9/12/444.
- [298] T. D. Kitching, A. N. Taylor, and A. F. Heavens. Systematic effects on dark energy from 3D weak shear. *MNRAS*, 389:173–190, September 2008. doi: 10.1111/j.1365-2966.2008.13419.x.
- [299] A. Refregier. The Dark UNiverse Explorer (DUNE): proposal to ESA’s cosmic vision. *Experimental Astronomy*, 23:17–37, March 2009. doi: 10.1007/s10686-008-9106-9.
- [300] E. Sellentin and B. M. Schäfer. Non-Gaussian forecasts of weak lensing with and without priors. *MNRAS*, 456:1645–1653, February 2016. doi: 10.1093/mnras/stv2805.
- [301] M. Feix, C. Fedeli, and M. Bartelmann. Asymmetric gravitational lenses in TeVeS and application to the bullet cluster. *A&A*, 480:313–325, March 2008. doi: 10.1051/0004-6361:20078224.
- [302] R. Reyes, R. Mandelbaum, U. Seljak, T. Baldauf, J. E. Gunn, L. Lombriser, and R. E. Smith. Confirmation of general relativity on large scales from weak lensing and galaxy velocities. *Nature*, 464:256–258, March 2010. doi: 10.1038/nature08857.
- [303] F. Simpson, C. Heymans, D. Parkinson, C. Blake, M. Kilbinger, J. Benjamin, T. Erben, H. Hildebrandt, H. Hoekstra, T. D. Kitching, Y. Mellier, L. Miller, L. Van Waerbeke, J. Coupon, L. Fu, J. Harnois-Déraps, M. J. Hudson, K. Kuijken, B. Rowe, T. Schrabback, E. Semboloni, S. Vafaei, and M. Velander. CFHTLenS: testing the laws of gravity with tomographic weak lensing and redshift-space distortions. *MNRAS*, 429:2249–2263, March 2013. doi: 10.1093/mnras/sts493.
- [304] C. Blake, S. Joudaki, C. Heymans, A. Choi, T. Erben, J. Harnois-Déraps, H. Hildebrandt, B. Joachimi, R. Nakajima, L. van Waerbeke, and M. Viola. RCSLenS: testing gravitational physics through the cross-correlation of weak lensing and large-scale structure. *MNRAS*, 456:2806–2828, March 2016. doi: 10.1093/mnras/stv2875.
- [305] M. Bartelmann. Cosmological parameters from angular correlations between QSOs and galaxies. *A&A*, 298:661–+, June 1995.
- [306] K. Dolag and M. Bartelmann. QSO-galaxy correlations induced by weak lensing in arbitrary Friedmann-Lemaître cosmologies. *MNRAS*, 291:446–+, November 1997.
- [307] R. Moessner and B. Jain. Angular cross-correlation of galaxies - A probe of gravitational lensing by large-scale structure. *MNRAS*, 294:L18–L24, February 1998.
- [308] R. Moessner, B. Jain, and J. V. Villumsen. The effect of weak lensing on the angular correlation function of faint galaxies. *MNRAS*, 294:291–+, February 1998.
- [309] A. C. C. Guimarães, C. van De Bruck, and R. H. Brandenberger. Galaxy-QSO correlation induced by weak gravitational lensing arising from large-scale structure. *MNRAS*, 325:278–286, July 2001.
- [310] B. Jain. Magnification Effects as Measures of Large-Scale Structure. *ApJL*, 580:L3–L6, November 2002.
- [311] A. J. Barber and A. N. Taylor. Shear and magnification angular power spectra and higher-order moments from weak gravitational lensing. *MNRAS*, 344:789–797, September 2003.
- [312] B. Ménard, T. Hamana, M. Bartelmann, and N. Yoshida. Improving the accuracy of cosmic magnification statistics. *A&A*, 403:817–828, June 2003.
- [313] M. Takada and T. Hamana. Halo model predictions of the cosmic magnification statistics: the full non-linear contribution. *MNRAS*, 346:949–962, December 2003.
- [314] M. Seldner and P. J. E. Peebles. Statistical analysis of catalogs of extragalactic objects. XI - Evidence of correlation of QSOs and Lick galaxy counts. *ApJ*, 227:30–36, January 1979.
- [315] W. Fugmann. Statistical gravitational lensing and the Lick catalogue of galaxies. *A&A*, 240:11–21, December 1990.
- [316] M. Bartelmann and P. Schneider. Largescale QSO - Galaxy Correlations Revisited. *A&A*, 271:421–+, April 1993.
- [317] M. Bartelmann and P. Schneider. Large-scale correlations between QSOs and galaxies - an effect caused by gravitational lensing? *A&A*, 268:1–13, February 1993.
- [318] M. Bartelmann and P. Schneider. Large-scale correlations between QSOs and IRAS galaxies. *A&A*, 284:1–11, April 1994.
- [319] M. Bartelmann, P. Schneider, and G. Hasinger. Diffuse X-ray emission around high-redshift, radio-loud QSOs. *A&A*, 290:399–411, October 1994.
- [320] A. Bartsch, P. Schneider, and M. Bartelmann. Reanalysis of the association of high-redshift 1-Jansky quasars with IRAS galaxies. *A&A*, 319:375–393, March 1997.
- [321] L. L. Rodrigues-Williams and C. J. Hogan. Statistical association of QSO’s with foreground galaxy clusters. *AJ*, 107:451–460, February 1994.
- [322] B. Fort, Y. Mellier, M. Dantel-Fort, H. Bonnet, and J.-P. Kneib. Observations of weak lensing in the fields of luminous radio sources. *A&A*, 310:705–714, June 1996.
- [323] I. Ferreras, N. Benítez, and E. Martínez-González. Are Optically-Selected QSO Catalogs Biased? *AJ*, 114:1728–+, November 1997.
- [324] L. L. R. Williams and M. Irwin. Angular correlations between LBQS and APM: weak lensing by the large-scale structure. *MNRAS*, 298:378–386, August 1998.
- [325] D. J. Norman and L. L. R. Williams. Weak Lensing-Induced Correlations between 1 JY QSOS and APM Galaxies on Angular Scales of a Degree. *AJ*, 119:2060–2067, May 2000.
- [326] N. Benítez, J. L. Sanz, and E. Martínez-González. Quasar-galaxy associations revisited. *MNRAS*, 320:241–248, January 2001.
- [327] S. M. Croom. QSO-Galaxy Correlations: Lensing or Dust? *Publications of the Astronomical Society of Australia*, 18:169–171, 2001.
- [328] D. J. Norman and C. D. Impey. Quasar-Galaxy Correlations: A Detection of Magnification Bias. *AJ*, 121:2392–2404, May 2001.
- [329] E. Gaztañaga. Correlation between Galaxies and Quasi-stellar Objects in the Sloan Digital Sky Survey: A Signal from Gravitational Lensing Magnification? *ApJ*, 589:82–99, May 2003.
- [330] B. Jain, R. Scranton, and R. K. Sheth. Quasar-galaxy and galaxy-galaxy cross-correlations: model predictions with realistic galaxies. *MNRAS*, 345:62–70, October 2003.
- [331] N. Benítez and J. L. Sanz. Measuring  $\Omega_B$  with Weak Lensing. *ApJL*, 525:L1–L4, November 1999.
- [332] B. Ménard and M. Bartelmann. Cosmological information from quasar-galaxy correlations induced by weak lensing. *A&A*, 386:784–795, May 2002.
- [333] B. Ménard and C. Péroux. Investigating lensing by absorbers in the 2dF-quasar survey. *A&A*, 410:33–43, October 2003.
- [334] B. Ménard, M. Bartelmann, and Y. Mellier. Measuring  $\Omega_0$  with higher-order quasar-galaxy correlations induced by weak lensing. *A&A*, 409:411–421, October 2003.

- [335] B. Ménard. Detecting and Interpreting Statistical Lensing by Absorbers. *ApJ*, 630:28–37, September 2005. doi: 10.1086/431728.
- [336] R. Scranton, B. Ménard, G. T. Richards, R. C. Nichol, A. D. Myers, B. Jain, A. Gray, M. Bartelmann, R. J. Brunner, A. J. Connolly, J. E. Gunn, R. K. Sheth, N. A. Bahcall, J. Brinkman, J. Loveday, D. P. Schneider, A. Thakar, and D. G. York. Detection of Cosmic Magnification with the Sloan Digital Sky Survey. *ApJ*, 633:589–602, November 2005. doi: 10.1086/431358.
- [337] B. Ménard, D. Nestor, D. Turnshek, A. Quider, G. Richards, D. Che-louche, and S. Rao. Lensing, reddening and extinction effects of MgII absorbers from  $z = 0.4$  to 2. *MNRAS*, 385:1053–1066, April 2008. doi: 10.1111/j.1365-2966.2008.12909.x.
- [338] H. Hildebrandt, L. van Waerbeke, and T. Erben. CARS: The CFHTLS-Archive-Research Survey. III. First detection of cosmic magnification in samples of normal high- $z$  galaxies. *A&A*, 507:683–691, November 2009. doi: 10.1051/0004-6361/200912655.
- [339] L. van Waerbeke. Shear and magnification: cosmic complementarity. *MNRAS*, 401:2093–2100, January 2010. doi: 10.1111/j.1365-2966.2009.15809.x.
- [340] F. Schmidt, A. Leauthaud, R. Massey, J. Rhodes, M. R. George, A. M. Koekemoer, A. Finoguenov, and M. Tanaka. A Detection of Weak-lensing Magnification Using Galaxy Sizes and Magnitudes. *ApJ*, 744:L22, January 2012. doi: 10.1088/2041-8205/744/2/L22.
- [341] A. Heavens, J. Alsing, and A. H. Jaffe. Combining size and shape in weak lensing. *MNRAS*, 433:L6–L10, June 2013. doi: 10.1093/mnras/slt045.
- [342] C. A. J. Duncan, B. Joachimi, A. F. Heavens, C. Heymans, and H. Hildebrandt. On the complementarity of galaxy clustering with cosmic shear and flux magnification. *MNRAS*, 437:2471–2487, January 2014. doi: 10.1093/mnras/stt2060.
- [343] J. Alsing, D. Kirk, A. Heavens, and A. H. Jaffe. Weak lensing with sizes, magnitudes and shapes. *MNRAS*, 452:1202–1216, September 2015. doi: 10.1093/mnras/stv1249.
- [344] B. R. Gillis and A. N. Taylor. A generalized method for measuring weak lensing magnification with weighted number counts. *MNRAS*, 456:2518–2536, March 2016. doi: 10.1093/mnras/stv2737.
- [345] L. Cayon, E. Martinez-Gonzalez, and J. L. Sanz. Gravitational lensing and the cosmic microwave background. *ApJ*, 403:471–475, February 1993. doi: 10.1086/172218.
- [346] L. Cayon, E. Martinez-Gonzalez, and J. L. Sanz. Does a cosmological constant increase the effect of gravitational lensing on the cosmic microwave background? *ApJ*, 413:10–13, August 1993. doi: 10.1086/172971.
- [347] U. Seljak. Gravitational Lensing Effect on Cosmic Microwave Background Anisotropies: A Power Spectrum Approach. *ApJ*, 463:1–+, May 1996. doi: 10.1086/177218.
- [348] U. Seljak and M. Zaldarriaga. A Line-of-Sight Integration Approach to Cosmic Microwave Background Anisotropies. *ApJ*, 469:437–+, October 1996. doi: 10.1086/177793.
- [349] F. Bernardeau. Weak lensing detection in CMB maps. *A&A*, 324:15–26, August 1997.
- [350] E. Martinez-Gonzalez, J. L. Sanz, and L. Cayon. The Effect of Weak Gravitational Lensing on the Cosmic Microwave Background Anisotropy: Flat versus Open Universe Models. *ApJ*, 484:1–+, July 1997. doi: 10.1086/304319.
- [351] R. B. Metcalf and J. Silk. Gravitational Magnification of the Cosmic Microwave Background. *ApJ*, 489:1–+, November 1997. doi: 10.1086/304756.
- [352] F. Bernardeau. Lens distortion effects on CMB maps. *A&A*, 338:767–776, October 1998.
- [353] M. Maturi, M. Bartelmann, M. Meneghetti, and L. Moscardini. Gravitational lensing of the CMB by galaxy clusters. *A&A*, 436:37–46, June 2005. doi: 10.1051/0004-6361/20041785.
- [354] S. Hagstotz, B. M. Schäfer, and P. M. Merkel. Born-corrections to weak lensing of the cosmic microwave background temperature and polarization anisotropies. *MNRAS*, 454:831–838, November 2015. doi: 10.1093/mnras/stv1977.
- [355] J. Guzik, U. Seljak, and M. Zaldarriaga. Lensing effect on polarization in the microwave background: Extracting the convergence power spectrum. *PRD*, 62(4):043517–+, August 2000. doi: 10.1103/PhysRevD.62.043517.
- [356] W. Hu. Weak lensing of the CMB: A harmonic approach. *PRD*, 62(4):043007–+, August 2000. doi: 10.1103/PhysRevD.62.043007.
- [357] W. Hu. Mapping the Dark Matter through the Cosmic Microwave Background Damping Tail. *ApJL*, 557:L79–L83, August 2001. doi: 10.1086/323253.
- [358] A. Challinor and G. Chon. Geometry of weak lensing of CMB polarization. *PRD*, 66(12):127301–+, December 2002. doi: 10.1103/PhysRevD.66.127301.
- [359] M. Kesden, A. Cooray, and M. Kamionkowski. Weak lensing of the CMB: Cumulants of the probability distribution function. *PRD*, 66(8):083007–+, October 2002. doi: 10.1103/PhysRevD.66.083007.
- [360] C. M. Hirata and U. Seljak. Reconstruction of lensing from the cosmic microwave background polarization. *PRD*, 68(8):083002–+, October 2003. doi: 10.1103/PhysRevD.68.083002.
- [361] C. M. Hirata and U. Seljak. Analyzing weak lensing of the cosmic microwave background using the likelihood function. *PRD*, 67(4):043001–+, February 2003. doi: 10.1103/PhysRevD.67.043001.
- [362] T. Okamoto and W. Hu. Cosmic microwave background lensing reconstruction on the full sky. *PRD*, 67(8):083002–+, April 2003. doi: 10.1103/PhysRevD.67.083002.
- [363] A. Challinor and A. Lewis. Lensed CMB power spectra from all-sky correlation functions. *PRD*, 71(10):103010–+, May 2005. doi: 10.1103/PhysRevD.71.103010.
- [364] R. Stompor and G. Efstathiou. Gravitational lensing of cosmic microwave background anisotropies and cosmological parameter estimation. *MNRAS*, 302:735–747, February 1999. doi: 10.1046/j.1365-8711.1999.02174.x.
- [365] A. Lewis. Lensed CMB simulation and parameter estimation. *PRD*, 71(8):083008–+, April 2005. doi: 10.1103/PhysRevD.71.083008.
- [366] C. Carbone, V. Springel, C. Baccigalupi, M. Bartelmann, and S. Matarrese. Full-sky maps for gravitational lensing of the cosmic microwave background. *MNRAS*, 388:1618–1626, August 2008. doi: 10.1111/j.1365-2966.2008.13544.x.
- [367] C. Carbone, C. Baccigalupi, M. Bartelmann, S. Matarrese, and V. Springel. Lensed CMB temperature and polarization maps from the Millennium Simulation. *MNRAS*, 396:668–679, June 2009. doi: 10.1111/j.1365-2966.2009.14746.x.
- [368] L. Perotto, J. Bobin, S. Plaszczyński, J.-L. Starck, and A. Lavabre. Reconstruction of the cosmic microwave background lensing for Planck. *A&A*, 519:A4+, September 2010. doi: 10.1051/0004-6361/200912001.
- [369] K. M. Smith, O. Zahn, and O. Doré. Detection of gravitational lensing in the cosmic microwave background. *PRD*, 76(4):043510–+, August 2007. doi: 10.1103/PhysRevD.76.043510.
- [370] C. M. Hirata, S. Ho, N. Padmanabhan, U. Seljak, and N. A. Bahcall. Correlation of CMB with large-scale structure. II. Weak lensing. *PRD*, 78(4):043520–+, August 2008. doi: 10.1103/PhysRevD.78.043520.
- [371] Planck Collaboration, P. A. R. Ade, N. Aghanim, C. Armitage-Caplan, M. Arnaud, M. Ashdown, F. Atrio-Barandela, J. Aumont, C. Baccigalupi, A. J. Banday, and et al. Planck 2013 results. XVII. Gravitational lensing by large-scale structure. *A&A*, 571:A17, November 2014. doi: 10.1051/0004-6361/201321543.



[372] Planck Collaboration, P. A. R. Ade, N. Aghanim, M. Ashdown, J. Aumont, C. Baccigalupi, A. J. Banday, R. B. Barreiro, N. Bartolo, S. Basak, E. Battaner, K. Benabed, A. Benoit-Lévy, J.-P. Bernard, M. Bersanelli, P. Bielewicz, J. J. Bock, A. Bonaldi, L. Bonavera, J. R. Bond, J. Borrill, F. R. Bouchet, F. Boulanger, C. Burigana, R. C. Butler, E. Calabrese, J.-F. Cardoso, A. Catalano, H. C. Chiang, P. R. Christensen, D. L. Clements, S. Colombi, L. P. L. Colombo, C. Combet, B. P. Crill, A. Curto, F. Cuttaia, L. Danese, R. J. Davis, P. de Bernardis, G. de Zotti, J. Delabrouille, C. Dickinson, J. M. Diego, O. Doré, A. Ducout, X. Dupac, F. Elsner, T. A. Enßlin, H. K. Eriksen, F. Finelli, O. Forni, M. Frailis, A. A. Fraisse, E. Franceschi, S. Galeotta, S. Galli, K. Ganga, T. Ghosh, M. Giard, Y. Giraud-Héraud, E. Gjerløw, J. González-Nuevo, K. M. Górski, A. Gruppuso, J. E. Gudmundsson, D. L. Harrison, C. Hernández-Monteagudo, D. Herranz, S. R. Hildebrandt, A. Hornstrup, W. Hovest, G. Hurier, A. H. Jaffe, W. C. Jones, E. Keihänen, R. Keskitalo, T. S. Kisner, J. Knoche, L. Knox, M. Kunz, H. Kurki-Suonio, G. Lagache, A. Lähteenmäki, J.-M. Lamarre, A. Lasenby, M. Lattanzi, R. Leonardi, F. Levrier, P. B. Lilje, M. Linden-Vørnle, M. López-Caniego, P. M. Lubin, J. F. Macías-Pérez, B. Maffei, G. Maggio, D. Maino, N. Mandolesi, A. Mangilli, M. Maris, P. G. Martin, E. Martínez-González, S. Masi, S. Matarrese, P. R. Meinhold, A. Melchiorri, A. Mennella, M. Migliaccio, S. Mitra, M.-A. Miville-Deschênes, A. Moneti, L. Montier, G. Morgante, D. Mortlock, A. Moss, D. Munshi, J. A. Murphy, P. Naselsky, F. Nati, P. Natoli, C. B. Netterfield, H. U. Nørgaard-Nielsen, D. Novikov, I. Novikov, L. Pagano, F. Pajot, D. Paoletti, F. Pasian, G. Patanchon, O. Perdereau, L. Perotto, V. Pettorino, F. Piacentini, M. Piat, E. Pierpaoli, E. Pointecouteau, G. Polenta, G. W. Pratt, J. P. Rachen, M. Reinecke, M. Remazeilles, C. Renault, A. Renzi, I. Ristorcelli, G. Rocha, C. Rosset, M. Rossetti, G. Roudier, J. A. Rubiño-Martín, B. Rusholme, M. Sandri, D. Santos, M. Savelainen, G. Savini, D. Scott, L. D. Spencer, V. Stolyarov, R. Stompor, R. Sudiwala, R. Sunyaev, D. Sutton, A.-S. Suur-Uski, J.-F. Sygnet, J. A. Tauber, L. Terenzi, L. Toffolatti, M. Tomasi, M. Tristram, M. Tucci, J. Tuovinen, L. Valenziano, J. Valiviita, B. Van Tent, P. Vielva, F. Villa, L. A. Wade, B. D. Wandelt, I. K. Wehus, D. Yvon, A. Zacchei, and A. Zonca. Planck intermediate results. XLI. A map of lensing-induced B-modes. *ArXiv e-prints*, December 2015.